Gondwana Research 83 (2020) 183–200

Contents lists available at ScienceDirect

Gondwana Research

journal homepage: www.elsevier.com/locate/gr

Early Cretaceous mantle upwelling and melting of juvenile lower crust in the Middle-Lower Yangtze River Metallogenic Belt: Example from Tongshankou Cu-(Mo—W) ore deposit

Gaobin Chu [a,b], Huayong Chen [b,c,*], Trevor.J. Falloon [d,**], Jinsheng Han [b], Shitao Zhang [a,b], Jiamin Cheng [a,b], Xiaobo Zhang [e]

[a] *CAS Key Laboratory of Mineralogy and Metallogeny, Guangzhou Institute of Geochemistry, Chinese Academy of Sciences, Guangzhou 510640, China*
[b] *University of Chinese Academy of Sciences, Beijing 100049, China*
[c] *Guangdong Provincial Key Laboratory of Mineral Physics and Materials, Guangzhou 510640, China*
[d] *ARC Centre of Excellence in Ore Deposits (CODES), University of Tasmania, Private Bag 79, Hobart 7001, Australia*
[e] *Geological Survey of Hubei Province, Wuhan 430034, China*

ARTICLE INFO

Article history:
Received 5 October 2019
Received in revised form 12 February 2020
Accepted 13 February 2020
Available online 25 March 2020

Handling Editor: S. Kwon

Keywords:
Mafic microgranular enclave
Adakitic magma
Geochemistry
Juvenile lower crust remelting
Extensional mantle upwelling

ABSTRACT

The linkage between intracontinental extension and the Early Cretaceous Cu-Mo-W polymetallic metallogenesis in the Middle-Lower Yangtze River Belt (MLYRB) has long been a subject of controversy due to the lack of convincing petrogenetic evidence to identify the nature of magmatic sources and their geological histories during extensional mantle upwelling. Here we present new zircon U—Pb ages, isotopic and geochemical data for granodiorites, quartz diorites and mafic microgranular enclaves (MMEs) in the Tongshankou area. Comparing the MMEs with their host porphyries, the different ratios of incompatible elements and the similar formation ages, coupled with quenched margins and the xenocrysts in the MMEs, indicate that the MMEs was most likely formed by mixing between mafic magma and their host felsic magma. The MMEs share similar geochemical and isotopic characteristics with the Cretaceous mafic rocks from MLYRB, indicating that MMEs were mostly derived from an enriched lithospheric mantle source without adakitic characteristics. Mixing of a crustal melt derived by melting of an amphibolite bearing juvenile lower crust with a mantle melt derived from melting of enriched lithospheric mantle can account for the generation of the Tongshankou prophyries. The melting of juvenile mafic lower crust and enriched lithospheric mantle is suggested to be caused by upwelling of asthenospheric mantle and the reactivity of trans-lithospheric faults in the intracontinental extensional environment. Our results therefore highlight that juvenile mafic lower crust beneath the Yangtze plate is one of the likely source for ore-forming magmatic rocks in the Early Cretaceous.

1. Introduction

The Middle-Lower Yangtze River Belt (hereafter referred to as "MLYRB") is the most important Cu-Fe-Au-Mo-polymetallic metallogenic region in eastern China (Pan and Dong, 1999; Zhai et al., 1996). Located in the northeastern area of the Yangtze craton (Fig. 1A, B), it consists of seven mineralization districts (Edong, Jiurui, Anqing, Tongling, Luzong, Ningwu, and Ningzhen) and comprises >200 ore deposits. Many of the porphyry, skarn, skarn-porphyry and strata-bound deposits have adakitic geochemical affinities (Wang et al., 2003, 2004, 2006; Xu et al., 2002). In the Edong district (westernmost section of MLYRB), >90% of the Cu–Fe–Au–Mo ores are related to adakite-like intrusive rocks (Shu et al., 1992; Zhai et al., 1996). In the past two decades, the genesis of "adakitic" rocks in the MLYRB (also named "continental" or "C-type" adakitic rocks) has attracted increasing interest and debate, as the study of "adakitic" rocks may hold the key to understanding the evolution of continental crust and the generation of porphyry or porphyry-related deposits (Mungall, 2002; Oyarzún et al., 2001). These debates were mainly focused on the following two aspects, i.e., the magmatic process and the magma source. The enriched lithospheric mantle, which was proposed to be the source of the Early Cretaceous mafic rocks in the MLYRB, has also been proposed for the source of ore-forming "adakitic" magmas. But the emplacement time of the ore-forming "adakitic" magmas is ~10 Ma earlier than that of the Early Cretaceous mafic rocks (130-125 Ma, Xie et al., 2011a). The coeval

---

[*] Correspondence to: H. Y. Chen, University of Chinese Academy of Sciences, Beijing 100049, China.
[**] Corresponding author.
E-mail addresses: huayongchen@gig.ac.cn (H. Chen), trevor.falloon@utas.edu.au (T.J. Falloon).

https://doi.org/10.1016/j.gr.2020.02.004

mafic member is a very important evidence to help us to understand this puzzle. The mafic microgranular enclaves (hereafter referred to as "MMEs") present in the Tongshankou adakitic porphyries, and reported in this paper for the first time, may provide important information on the characteristics of magmas associated with the Tongshankou adakite porphyries and the role of enriched lithospheric mantle.

The Tongshankou Cu-Mo-W deposit, located in the southwest part of the Edong ore district (Fig. 1C), is a representative example of a porphyry-skarn type Cu–Mo-W deposits and an ore-forming adakitic magma in the MLYRB. Wang et al. (2004) proposed that the mineralized Tongshankou granodiorite porphyry was probably derived from partial melting of delaminated lower crust in the underlying lithospheric mantle. Li et al. (2008) suggested that Tongshankou granodiorite was formed by large-scale partial melting of enriched lithospheric mantle which had been metasomatized by slab melts related to an previous subduction event. In the comparitive study between ore-bearing and barren adakitic rocks in the east sections of the MLYRB, Li et al. (2013) suggested that the Tongshankou granodiorite was most likely generated by fractional crystallization of basaltic magma which was derived from an enriched mantle source metasomatized by melts of sediments.

In this paper, we present new zircon U—Pb ages, and isotopic and whole-rock geochemical data for the Tongshankou granodiorite, as well as the first detailed study on the coeval Tongshankou quartz diorite and MMEs, in order to understand: (1) the relative formation time of the Tongshankou porphyries and coeval MMEs; (2) the petrogenetic relationship between the MMEs and host rocks; and (3) their regional geodynamic implications.

2. Geological setting and Mesozoic magmatism

The MLYRB is located in the northeastern margin of Yangtze craton and to the south of the Qinling-Dabieshan orogenic belt (Fig. 1A, B). The northern boundary of this region is defined by the Xiangfan-Guangji and Tancheng-Lujiang faults, which together separate the MLYRB from Qinling-Dabieshan orogenic belt. The southern boundary is defined by the Yangxin-Changzhou Fault separating the MLYRB from the Yangtze craton (Fig. 1). The oldest basement rocks in the Yangtze craton, exposed in the Kongling area, is an upper amphibolite to granulite facies complex (the Kongling Group), consisting of amphibolites, metasedimentary rocks, high-grade metamorphic tonalites, trondhjemite and granodiorite gneisses (TTG) (Gao et al., 1999, 2011). The Kongling Group is mainly Meso- to Neoarchean with Rb—Sr, Sm—Nd, and zircon U—Pb ages of 2.6–2.9 Ga (Ames et al., 1996; Qiu et al., 2000). In contrast to the Yangtze craton, there are no Archean rocks exposed in the MLYRB. The oldest basement rock in MLYRB is the Dongling Group with Sm—Nd, and zircon U—Pb ages of 1.85–0.77 Ga (Chen and Xing, 2016; Wang and He, 2016). The Dongling Group is overlain by a continuous continental to neritic margin sedimentary sequence of Sinian (ca. 800–570 Ma) to the Lower Triassic age, composed by calc-alkaline basalts, rhyolites, and marine sedimentary rocks, except for a short break during the Early and Middle Devonian (Chen et al., 2001). In the Late Triassic, this region has undergone intense intraplate deformation with the development of NEE- or NE-trending composite folds and fault systems, due to the continental collision between the Yangtze and North China cratons. From the Upper Triassic to Holocene, the Yangtze block was continental and characterized by terrestrial sedimentary (such as coal-bearing shale and red-bed deposition), volcano-sedimentary sequences and intrusive rocks (Shu et al., 1992).

In the Edong district, the Jurassic strata are dominated by continental coal-bearing shale. Extensive magmatism and volcanism occurred in the Early Cretaceous, characterized by the Majiashan, Lingxiang, Dasi and Taihe formation volcanic rocks in the Jinniu volcanic basin and several associated intrusive complexes (Xie et al., 2006, 2011a). The intrusive rocks are hosted by Silurian to Early Triassic sedimentary rocks, and comprise six major plutons (from north to south, the Echeng, Tieshan, Jinshandian, Lingxiang, Yangxin, and Yinzu plutons) and over 100 smaller stocks (Fig. 1C). The Tongshankou granodiorite porphyry, one of the smaller stocks, together with another two small stocks (Longjiaoshan-Fujiashan granodiorite porphyry and the Ruanjiawan quartz diorite) are related to porphyry Cu-W-(Mo) mineralization with zircon U—Pb ages of ca. 147–143 Ma (Ding et al., 2014; Li et al., 2010; Yan et al., 2012). The Yangxin pluton, located in the southwest of Edong district, is dominated by medium-grained quartz diorite. Cu-Au-Fe mineralization, such as the Tonglvshan Cu–Au–(Fe) deposit and the Jiguangzui Cu—Au deposit are associated with the Yangxin pluton and have zircon U—Pb ages of ca. 141–138 Ma (Li et al., 2009; Li et al., 2010; Xie et al., 2011c; Zhang et al., 2018). The other major plutons including the Lingxiang diorite and quartz diorite (in the southeast), the Jinshandian quartz diorite and diorite (in the east), the Tieshan quartz diorite (in the northeast) and the Echeng granite and monzonite (in the north) are all related to Fe mineralization, called the "Daye-type" skarn Fe (Cu, Co, S) mineralization, with ages of 135–123 Ma (Fig. 1C; Li et al., 2009; Zhou et al., 2015), except for the Lingxiang pluton which has older zircon U—Pb ages of ca. 145 Ma (Li et al., 2010). The large barren Yinzu pluton in the southwestern of Edong district is dominated by medium-grained quartz diorite with zircon U—Pb age of ca. 152–146 Ma (Li et al., 2009; Li et al., 2010).

3. Geology and petrology of the Tongshankou intrusive complex

The Tongshankou Cu-Mo-W deposit is located at the southeast part of the Edong district, about 20 km away from Daye city (Fig. 1C). It is a large skarn-porphyry deposit, containing a total proven reserve of 64.156 Mt. at 0.86% Cu, 9.731 Mt. at 0.104% Mo and 6.612 Mt. at 0.185% WO_3 by the end of 2018. The Tongshankou granodiorite porphyry intruded into the limestone and dolomite of the Lower Triassic Daye Formation (4th, 5th and 6th layer; Li et al., 2008; Xia et al., 2015; Zhou et al., 2015) and formed six orebodies with a few smaller Mo ore-bodies (Fig. 2). Li et al. (2008) reported that six molybdenite samples from the porphyry ores yielded a Re—Os isochron age of 143.8 ± 2.6 Ma (2σ), and a phlogopite sample from the skarn ores yielded an $^{40}Ar/^{39}Ar$ plateau age of 143.0 ± 0.3 Ma with an isochron age of 143.8 ± 0.8 Ma (2σ), confirming that the Tongshankou mineralization occurred at about 143 Ma. The crystallization ages of the Tongshankou granodiorie porphyry has been previously determined by a number of studies with ages ranging from approximately 140–144 Ma. These ages were determined by a range of different techniques including SHRIMP U—Pb (140.6 ± 2.4 Ma, Li et al., 2008), SIMS (144.0 ± 1.3 Ma, Li et al., 2010) and LA-ICP-Ms (143.5 ± 0.45 Ma, Xia et al., 2015), all of which are generally, consistent with the determined mineralization ages.

The Tongshankou granodiorite porphyry is separated by fault (F6) which divides the porpyry into the Shizishan stock (west) and the Tongshankou stock (east), with a total outcrop area of approximately 0.33 km^2 (Li et al., 2008; Zhou et al., 2015; Fig. 2). The granodiorite porphyry (Fig. 3A) contains abundant phenocrysts (5–15 mm, 40–50 vol%) consisting of plagioclase (25–30 vol%), quartz (10 vol%) and orthoclase (5 vol%), with minor biotite (5–10 vol%) and hornblende (5 vol%). Minerals in the groundmass (50–60 vol%) are phanerocrystalline (fine-grained, generally <50 μm), and mainly consist of plagioclase (25–30 vol%), quartz (10 vol%), K-feldspar (<5 vol%), and biotite (<5 vol%). Accessory minerals include titanite, magnetite, apatite and zircon (Fig. 3D). The Tongshankou granodiorite is intruded by a quartz

Fig. 1. (a) A simplified geological map of China (modified from Mao et al., 2011). (b) Geological map of magmatic rocks and deposits in the Middle-Lower Yangtze River Valley Metallogenic Belt (modified from Chang et al., 1991; Mao et al., 2011). TLF:Tancheng-Lujiang fault, XGF: Xiangfan-Guangji fault, YCF: Yangxing-Changzhou fault. (c) Geological map of the Edong district, showing mineralization types (modified from Xie et al., 2011a, 2011b, 2011c).

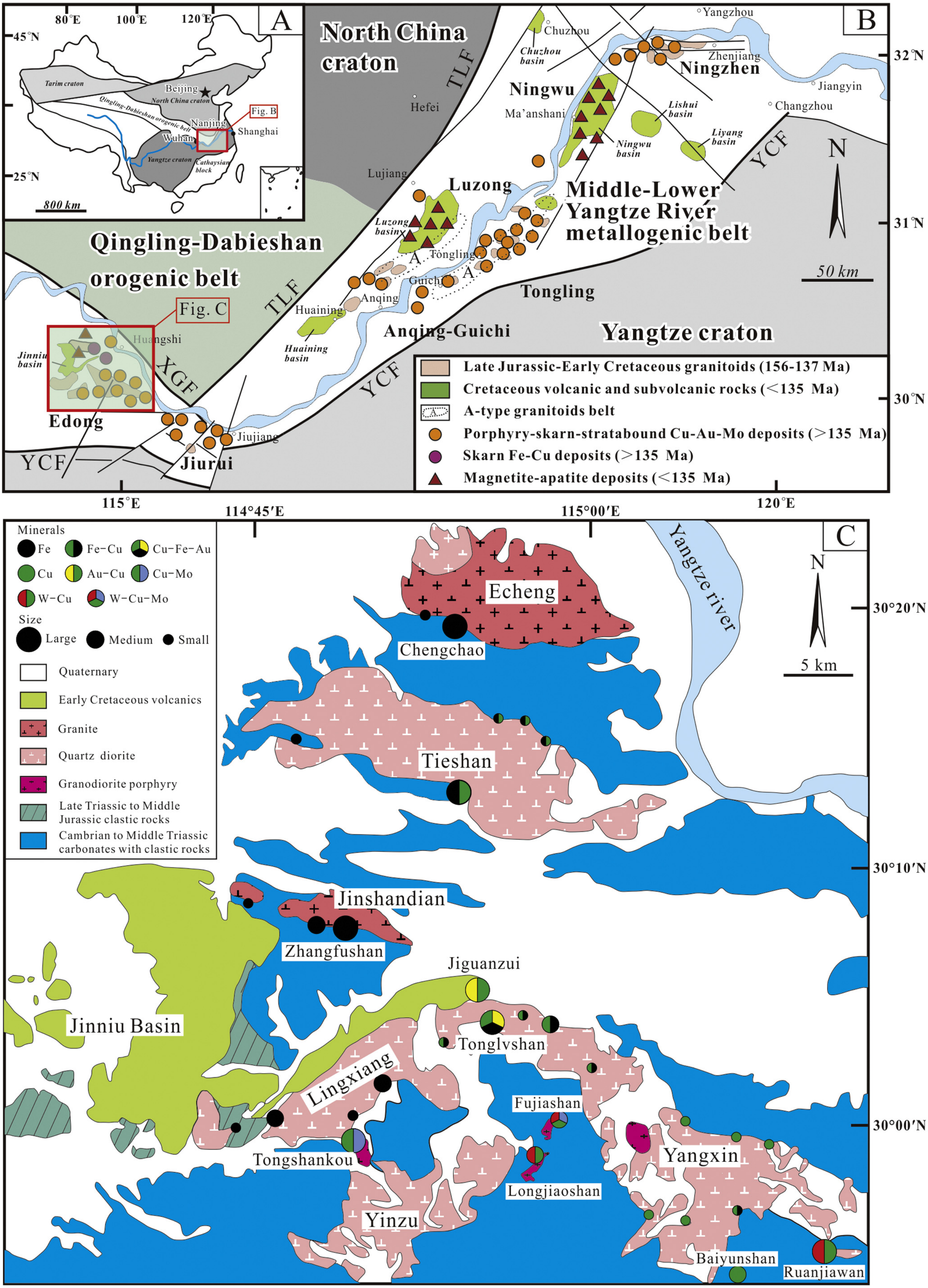
A
80°E
100°E
120°E
45°N
25°N
Tarim craton
Beijing
North China craton
Qingling-Dabieshan orogenic belt
Nanjing
Fig. B
Shanghai
Wuhan
Yangtze craton
Cathaysian block
800 km
B
North China craton
TLF
Hefei
Chuzhou
Chuzhou basin
Yangzhou
Zhenjiang
Ningzhen
32°N
Jiangyin
Changzhou
Ningwu
Ma'anshan
Lishui basin
Liyang basin
Ningwu basin
YCF
N
Lujiang
Luzong
Luzong basin
Middle-Lower Yangtze River metallogenic belt
31°N
Tongling
Guichi
Anqing
A
50 km
Qingling-Dabieshan orogenic belt
Fig. C
Huaining
Huaining basin
Tongling
Anqing-Guichi
Yangtze craton
Huangshi
Jinniu basin
XGF
Edong
YCF
Jiujiang
Jiurui
30°N
115°E
120°E
Late Jurassic-Early Cretaceous granitoids (156-137 Ma)
Cretaceous volcanic and subvolcanic rocks (<135 Ma)
A-type granitoids belt
Porphyry-skarn-stratabound Cu-Au-Mo deposits (>135 Ma)
Skarn Fe-Cu deposits (>135 Ma)
Magnetite-apatite deposits (<135 Ma)
114°45′E
115°00′E
C
Minerals
Fe
Fe-Cu
Cu-Fe-Au
Cu
Au-Cu
Cu-Mo
W-Cu
W-Cu-Mo
Size
Large
Medium
Small
Quaternary
Early Cretaceous volcanics
Granite
Quartz diorite
Granodiorite porphyry
Late Triassic to Middle Jurassic clastic rocks
Cambrian to Middle Triassic carbonates with clastic rocks
Echeng
Chengchao
Yangtze river
N
5 km
30°20′N
Tieshan
30°10′N
Jinshandian
Zhangfushan
Jiguanzui
Jinniu Basin
Tonglvshan
Lingxiang
Fujiashan
30°00′N
Yangxin
Tongshankou
Longjiaoshan
Yinzu
Baiyunshan
Ruanjiawan

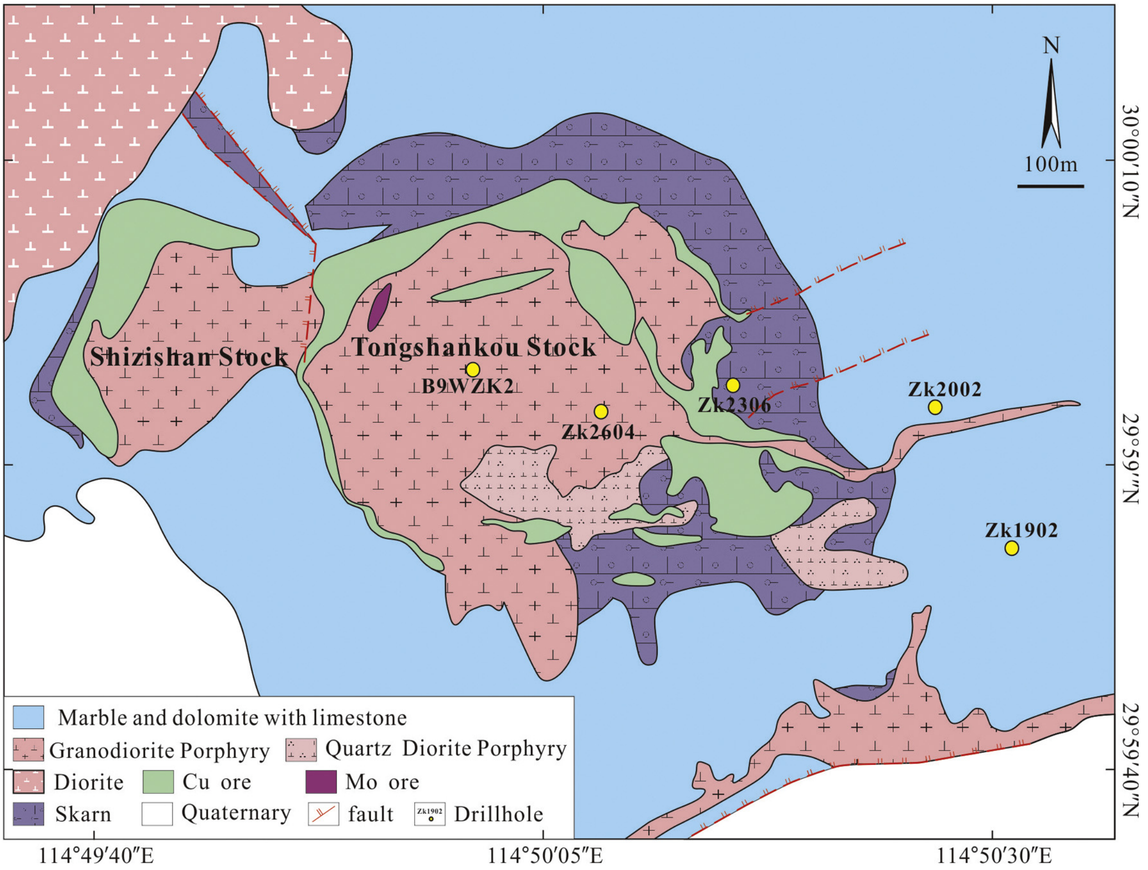

Fig. 2. Geological map of the Tongshankou deposit with the drillhole locations (modified after Li et al., 2008).

diorite stock as evidenced by drill core samples (Fig. 3C). The quartz diorite has a porphyritic texture (Fig. 3B), containing phenocrysts (35–40 vol%, 2–10 mm) of plagioclase (20–25 vol%), quartz (5–10 vol%) and hornblende (10 vol%), with minor biotite (5 vol%) and orthoclase (<5 vol%). The groundmass of the quartz diorite is cryptocrystalline, and consists mainly of felsic minerals. Accessory minerals include titanite, apatite and zircon (Fig. 3E). The MMEs in both the Tongshankou granodiorite and quartz diorite porphyry from the deep drill core samples (below 300 m) have been identified for the first time in this study. The MMEs in Tongshankou are ellipsoidal, spindle-shaped or elongate, and exhibiting a fine granular texture (Fig. 3F and G). These MMEs consist of euhedral-subhedral hornblende, biotite, plagioclase. Accessory minerals include titanite, apatite, magnetite and zircon (Fig. 3H and I).

4. Sampling and results

The samples for this study were collected from five different drill cores and their detailed information is listed in the Supplementary Table S1. Detailed analytical methods of whole-rock major and trace element, Sr—Nd isotopes and zircon U—Pb dating, Lu—Hf isotope composition are given in supplementary the Supplementary Text S1.

4.1. Whole rock major and trace element geochemistry

The chemical compositions of all samples are reported in the Supplementary Table S2 and illustrated in Figs. 4 and 5. Three samples from the Tongshankou granodiorite porphyry and two samples from the Tongshankou quartz diorite porphyry exhibit intermediate–felsic compositions. Compared with the MMEs in the Tongshankou and the high-MgO low-silica adakitic rocks around the world, they have relatively low concentrations of MgO with low Mg# values [Mg# = molecule MgO/(MgO + FeO_T) × 100]. They also show high contents of Na_2O, K_2O and Al_2O_3, with high A/NK values and low A/CNK values, indicating that the Tongshankou granodiorite and quartz diorites are both metaluminous and high-K calc-alkaline in nature (Fig. 4B). Both of the porphyries are enriched in large-ion lithophile elements (LILE, including Rb, Ba, Th, U, Sr and Pb), depleted in high field strength elements (HFSE, such as Nb, Ta and Ti) and have low concentrations of Cr, Ni and Y (Fig. 5A). Chondrite-normalized rare earth element (REE) patterns show that all samples are enriched in light REE (LREE) and depleted in heavy REE (HREE) with high $(La/Yb)_N$ valuesand no obvious Eu anomalies (Fig. 5B).

Six analyzed samples of the MMEs exhibit alkaline compositions. Compared with their host rocks, they have a wide range of SiO_2 content (43.20–54.37 wt%) and relatively high concentrations of MgO (2.66–4.61 wt%) with high Mg# values (42–48). These samples have high concentrations of Na_2O, K_2O, and as can be seen in Fig. 4A, define a range of magmatic affinities from medium-K calcalkaline to shoshonitic in nature (Fig. 4B). They are enriched in LILE, depleted in HFSE and have high concentrations of Cr (25–88 ppm), Ni (12–36 ppm) and Y (19.1–61.2 ppm) (Fig. 5A). And They share similar chondrite-normalized REE patterns with their host porphyries, but with high contents of Yb, and have low but variable $(La/Yb)_N$ values (14–99) and no obvious Eu anomalies (Eu/Eu* = 0.81–1.00) (Fig. 5B).

4.2. Whole rock Sr and Nd isotopes

The Sr—Nd isotopic data of the studied rocks are reported in the Supplementary Table S2. The initial $^{87}Sr/^{86}Sr$ ratios and εNd(t) values of the granodiorites and quartz diorites have been calculated using an age of 143 Ma on the basis of the zircon U—Pb ages (see below). The analyzed samples of the granodiorite porphyry span a narrow range of initial $^{87}Sr/^{86}Sr$ values (0.7061–0.7063) and εNd(t) values(−5.7 to −5.0). The quartz diorite porphyry samples also have a narrow range of initial

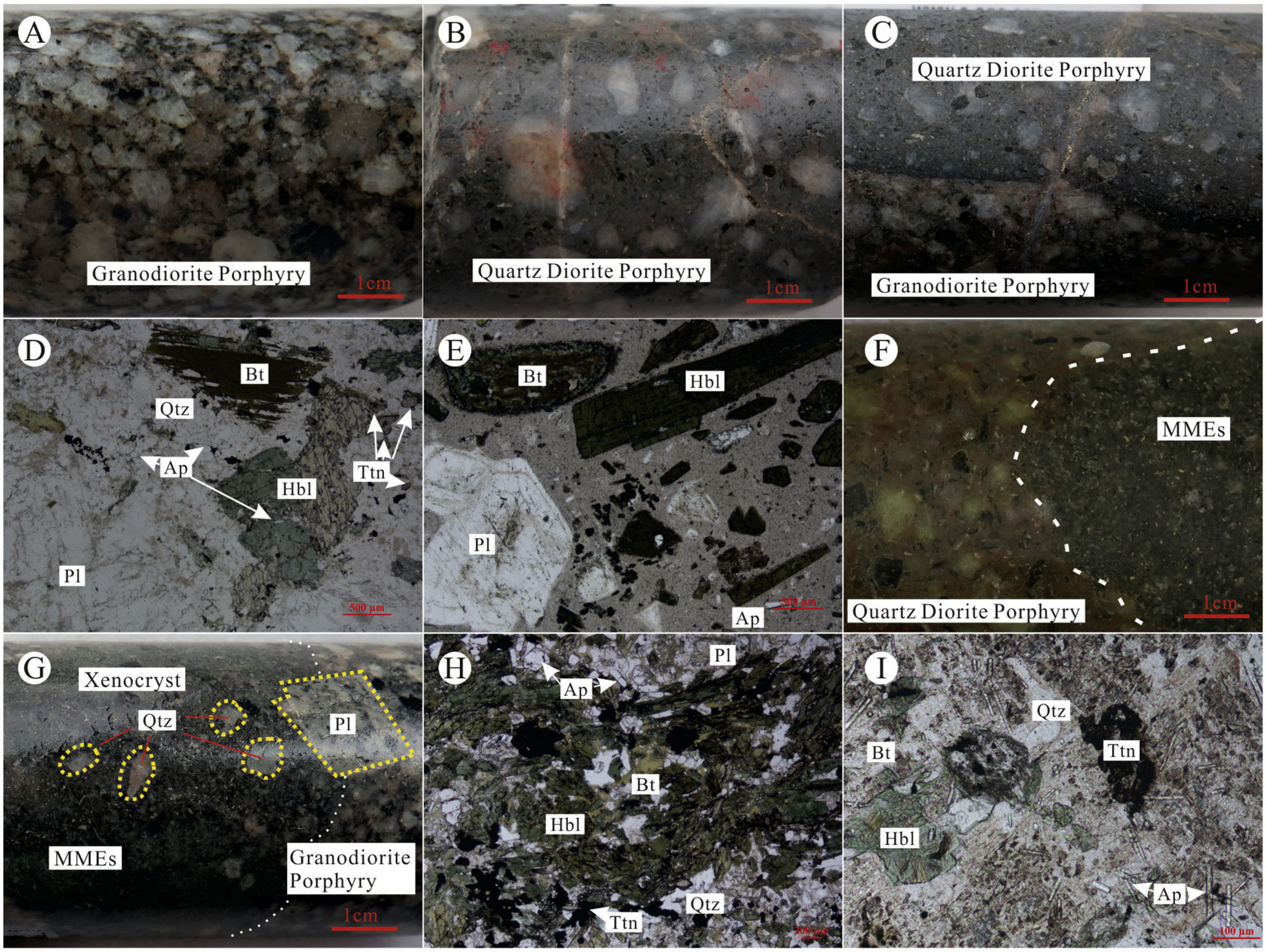

Fig. 3. Representative photographs and photomicrographs of the rock types in the Tongshankou deposit. (a) Tongshankou granodiorite porphyry (drill-hole sample). (b) Tongshankou quartz diorite porphyry (drill-hole sample). (c) The contact relationship between the Tongshankou granodiorite porphyry and quartz diorite porphyry (drill-hole sample). (d) Photomicrographs of Tongshankou granodiorite porphyry. (e) Photomicrographs of Tongshankou quartz diorite porphyry. (f) MMEs hosted in the Tongshankou quartz diorite porphyry (drill-hole sample). (g) MMEs with quartz and plagioclase xenocrysts within the Tongshankou granodiorite porphyry (drill-hole sample). (h) Photomicrographs of Tongshankou MMEs with fine-grained dark mineral assemblages. (i) Photomicrographs of Tongshankou MMEs with minor acicular apatite. Abbreviations: Qtz = quartz, Bt = biotite, Ttn = titanite, Pl = plagioclase, Ap = apitite, Hbl = hornblende.

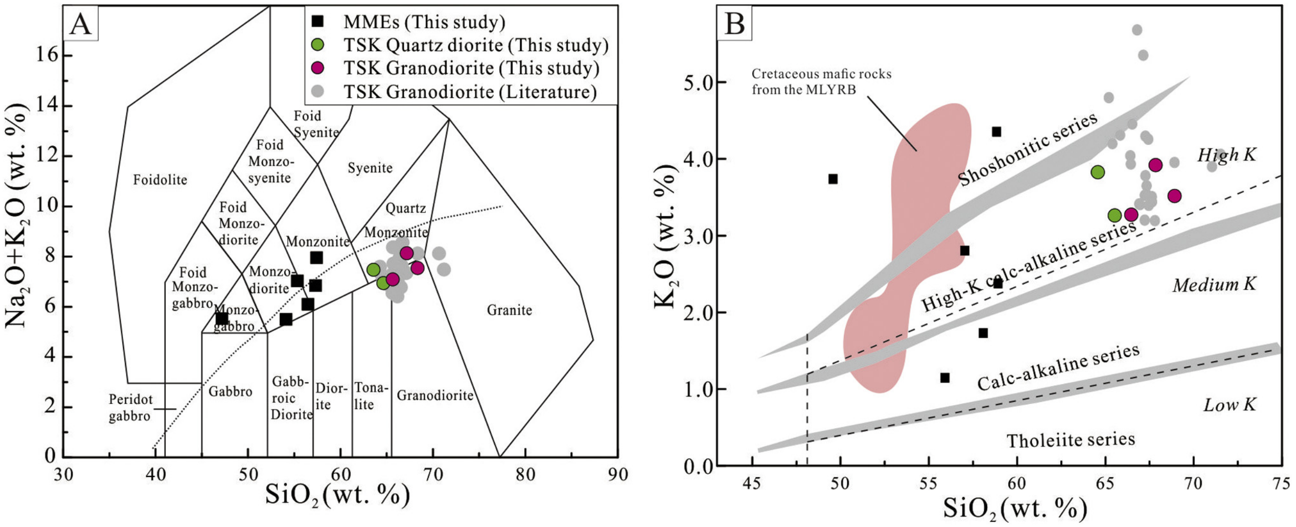

Fig. 4. (a) Total alkali versus silica (TAS) plot for the samples from Tongshankou deposit (Le Maitre, 1989). All the major element data were recalculated to 100% volatile free. The line separating alkali basalts and tholeiites is from Irvine and Baragar (1971). (b) K_2O versus SiO_2 (Peccerillo and Taylor, 1976), data field of the Cretaceous mafic rocks from the MLYRB are after Xie et al. (2006), Wang et al. (2006), Yan et al. (2008) and Yuan et al. (2008); data with gray solid gray dots of the Tongshankou granodiorite are from Wang et al. (2004), Li et al. (2008) and Li et al. (2013).

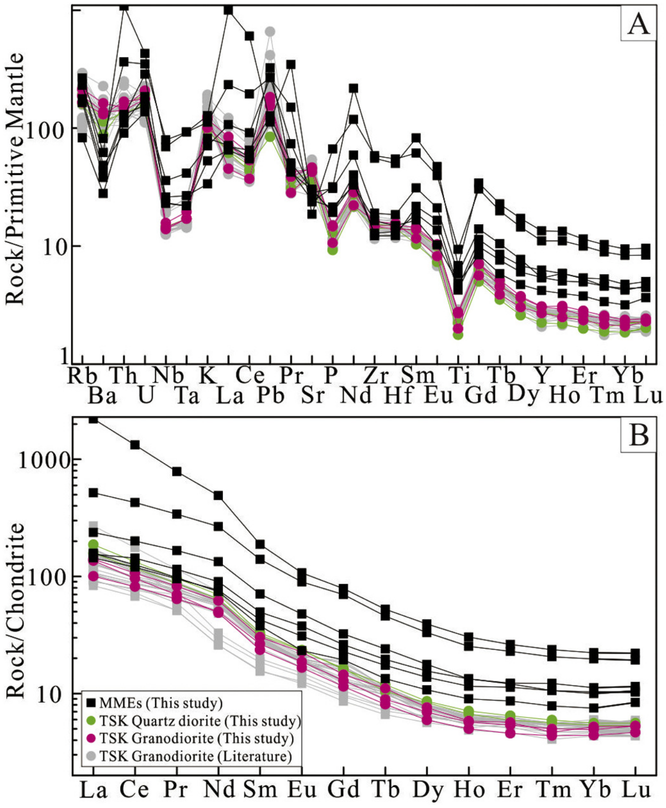

Fig. 5. (a) Primitive mantle-normalized multi-element diagrams for the samples from Tongshankou deposit. The primitive mantle normalizing values are from Sun and McDonough (1989). (b) Chondrite-normalized rare earth element patterns for the rocks from Tongshankou deposit. The Chondrite-normalized values are from Boynton (1984).

$^{87}Sr/^{86}Sr$ values (0.7061 and 0.7064) and εNd(t) values(−5.7 and −5.4) similar to the granodiorite. The initial $^{87}Sr/^{86}Sr$ ratios and εNd(t) values of MMEs were calculated using the crystallization age of 145 Ma. The analyzed MMEs samples span a larger range of initial $^{87}Sr/^{86}Sr$ values from 0.7057 to 0.7073, while εNd(t) values in contrast show a relatively narrow range from −5.7 to −4.7.

4.3. Zircon U—Pb geochronology

All the LA–ICP-MS zircon U—Pb data are presented in the Supplementary Table S3. The zircon of granodiorite porphyry sample (G4) has euhedral or irregular zircons that are 110 to 300 μm long with length/width values between 2:1 and 3:1 (Fig. 6A). They have Th/U values of 0.23 to 0.52 and oscillatory growth zonation in the rim and cores, suggesting a magmatic origin (Hoskin and Schaltegger, 2003). Thirty-five analyses on zircons yielded a weighted mean age of 143.9 ± 0.6 Ma (1σ, MSWD = 1.6; Fig. 6B), which is interpreted to be the crystallization age for the pluton.

Zircons from quartz diorite porphyry sample QD2 are euhedral or irregular. The grains are 100–200 μm long with length/width values of 1:1 to 2:1. They have Th/U values of 0.21 to 0.45 and show clear oscillatory zoning (Fig. 6C), suggesting a magmatic origin. The twenty-nine analyses yielded a weighted mean age of 143.6 ± 0.7 Ma (1σ, MSWD = 1.9; Fig. 6D), which is interpreted to be the crystallization age for the pluton.

The MMEs sample S4, zircon crystals are euhedral, ranging from 100 to 3000 μm in size, with length/width values of 2:1 to 4:1 (Fig. 6E). They have Th/U values of 0.18 to 0.35 and characteristic oscillatory growth zoning, suggesting a magmatic origin. Seventeen analyzed zircons yielded a weighted mean age of 145.4 ± 1.9 Ma (1σ, MSWD = 1.6; Fig. 6F), which is interpreted to be the crystallization age for the MMEs in both of the two plutons.

4.4. Zircon Lu—Hf isotopes

The Lu—Hf isotope results are listed in the Supplementary Table S4. The zircons from the granodiorite porphyry (G4) have variable Hf-isotope compositions, with initial $^{176}Hf/^{177}Hf$ values from 0.282498 to 0.282555 and εHf(t) values from −6.5 to −4.5. Their depleted mantle Hf model ages (T_{DM}) range from 0.98 to 1.06 Ga, with crustal model ages (T_{DM}^{C}) from 1.48 to 1.61 Ga. Zircons from the quartz diorite porphyry (QD2) have variable Hf-isotope compositions, with initial $^{176}Hf/^{177}Hf$ values from 0.282403 to 0.282533 and εHf(t) values from −9.9 to −5.3. Their T_{DM} ages range from 1.01 to 1.20 Ga with T_{DM}^{C} of 1.53 to 1.82 Ga. Zircons from the MME sample (S4) have variable Hf-isotope compositions, with initial $^{176}Hf/^{177}Hf$ values from 0.282387 to 0.282513 and εHf(t) values from −10.2 to −6.1. Their T_{DM} ages range from 1.03 to 1.22 Ga with T_{DM}^{C} of 1.58 to 1.85 Ga.

5. Discussion

5.1. Origin of the MMEs

MMEs are widespread in intermediate-felsic intrusions. Recent years, other researchers also found some MMEs at Tongling district in MLYRB (Du et al., 2007; Wang et al., 2016).

MMEs could be generated from several different processes: (a) restites: the recrystallized and residual phase assemblages, in other words the refractory components derived from the sources of the host rocks (e.g., Chappell and White, 1992; Chappell et al., 1987); (b) autoliths: the chilled material or cumulate mineral assemblages formed during the early stages of magma evolution from the same magma source as the host rocks (e.g., Chappell et al., 1987; Tindle and Pearce, 1983); (c) xenoliths: the solid country rocks, incorporated during the emplacement and/or crystallization process of their host magma (e.g., Bacon, 1986; Maas et al., 1997; Vernon, 1983); and (d) quenched inclusions: the products of mixing between mafic and their host felsic magma in different proportions (e.g., Vernon, 1984; Holden et al., 1987; Kent et al., 2010; Zhao et al., 2012).

Within error, the formation age of Tongshankou MMEs is in agreement with their host rocks, indicating that the enclaves are unlikely to be the restites of the source rock to the host porphyries. As for a xenolithic origin, the most likely source would be regional lithological units. In this district, only the Yinzu and Yangxin adakitic rocks share similar ages with the Tongshankou MMEs, but they have clearly different structure, texture, mineral compositions and geochemical composition (Fig. 9A). Therefore, the MMEs in the Tongshankou are neither restites nor xenoliths. Furthermore, at Tongshankou, we found plagioclase megacrysts crossing the boundary of MMEs (Fig. 3G). There is also quartz ocelli (Fig. 3G) with embayed boundary surrounded by fine-grained dark mineral assemblages in some MMEs, which indicates that quartz xenocrysts derived from the host felsic magma have been thermally eroded by relatively high-temperature mafic magma. Moreover, the MMEs usually have quenched margin with fine-grained dark mineral assemblages (Figs. 3F, H) and minor acicular apatite (Fig. 3I), indicating rapid reducing of the mafic magma temperature and subsequent crystallization (Wyllie et al., 1962). These above phenomena indicate that the temperature of the MMEs magma system is much higher than the surrounding magma during the formation of the MMEs, inconsistent with the balanced and continuously variable temperature of the magma during the formation of autoliths through fractional crystallization process (Keith et al., 1997). These special textures, mineral assemblages and chemical characteristics strongly indicate that the Tongshankou MMEs were formed by magma mixing process. The SiO_2 content difference betwen the MMEs (43.20–54.37 wt%) and their host porphyries (61.82–66.35 wt%) is much higher than the maximum SiO2 content (10%) for a

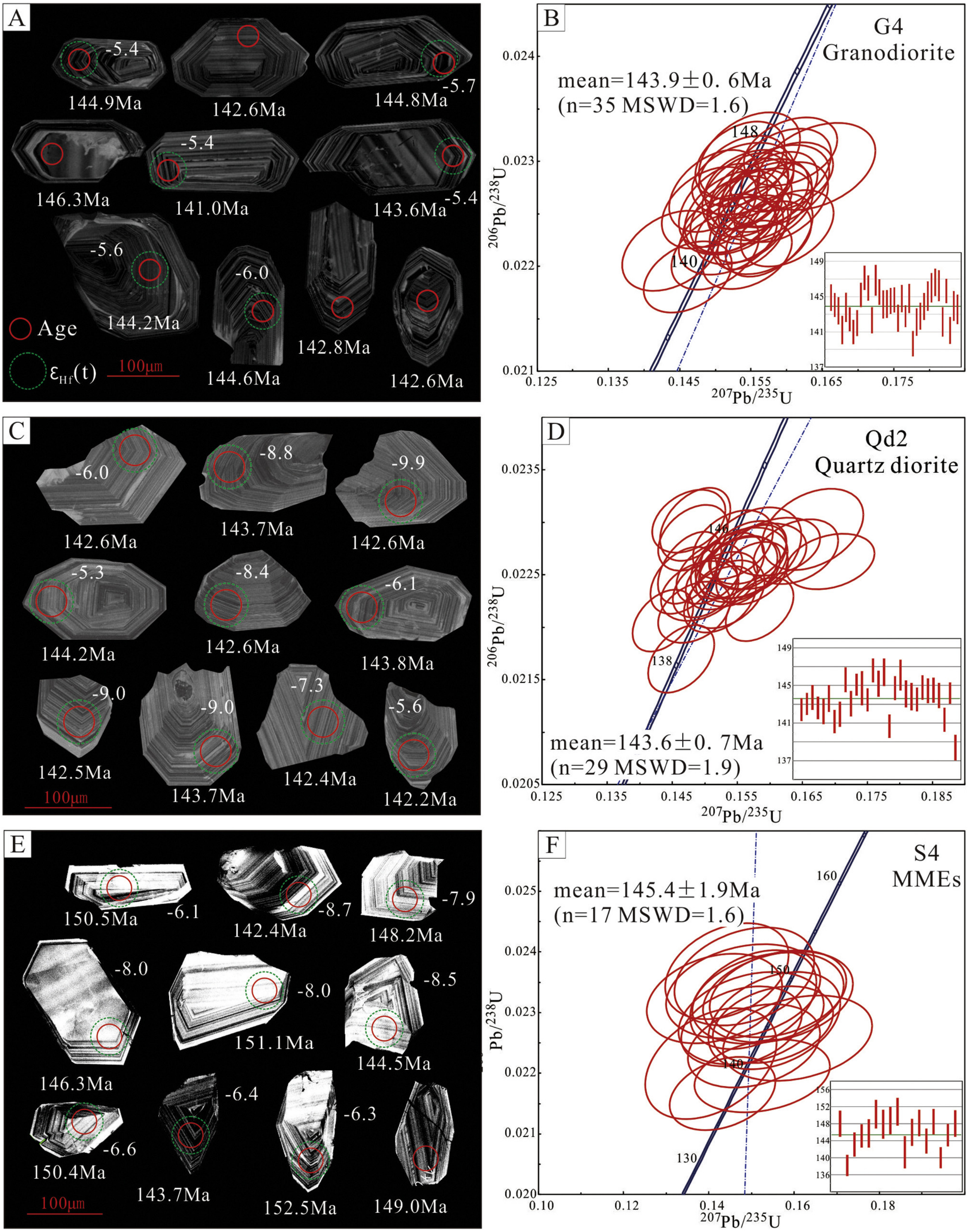

Fig. 6. (a) (c) (e) Representative zircon CL images and analyzed spots with U—Pb ages and Lu—Hf isotope data. (b) (d) (f)Concordia plots and age data bar charts for zircon LA–ICP-MS U—Pb data from the Tongshankou deposit.

homogenous mixing, so the small amounts of mafic magmas were not totally mixed to form a homogenous magma but formed the Tongshankou MMEs (Frost and Mahood, 1987).

The chemical composition of MMEs shows a large variation, however, their data points show a linear trend on the harker diagrams towards the field of their host rocks (Fig. 7A–D), consistent with

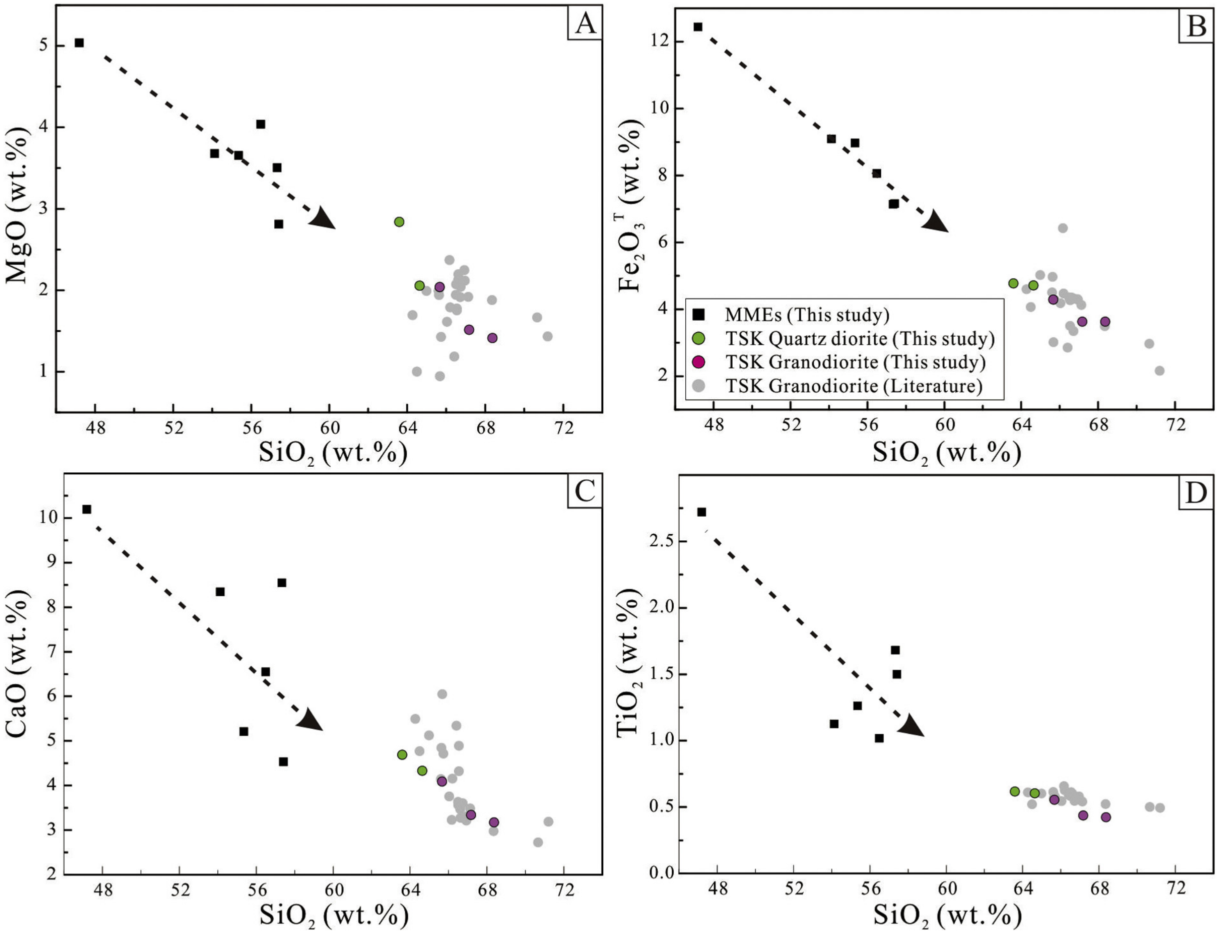

Fig. 7. Harker diagrams of the samples from Tongshankou deposit(a-d). The linear trends of MMEs (from the most basic point to the field of Tongshankou porphyries) indicate the influence of magma mixing process.

mixing of mafic and felsic magmas, which can account for the chemical linear trend changes of MMEs due to mass balance between small amount of mafic magma and its host felsic rocks (e.g., Blundy and Sparks, 1992; Dodge and Kistler, 1990; Frost and Mahood, 1987; Fu et al., 2016; Liao et al., 2013). This conclusion is also supported by the similar REE patterns of the MMEs and their host felsic rocks (Fig. 5).

The comparation of the compositions between the MMEs in the Tongshankou and the mafic rocks in the MLYRB can help us get an approximate constraint on the source of the MMEs. Their low content of TiO_2 (<2.50 wt%), high content of Y (>19 ppm), enrichment in LILE and strong depletions of HFSE are very similar to normal arc magmas (Figs. 9A, B), which suggests a hydrous mantle source metasomatized by fluids/melts derived from the subducted oceanic plate (Schmidt et al., 2004; Tasumi et al., 1986). Furthermore, their high contents of MgO (2.66–4.61 wt%) with Mg# of 42 to 48, high concentrations of Ni (12–36 ppm) and Y (19.1–61.2 ppm) are very similar to the Cretaceous mafic rocks from MLYRB (137–124 Ma, Xie et al., 2006; Xu and Xing, 1994; Zhou et al., 2008). Yan et al. (2008) proposed that the Cretaceous MLYRB mafic rocks could be divided into the northeastern and southwestern groups. The southwestern group (similar to the Tongshankou MMEs) was considered to have been derived from an isotopically enriched lithospheric mantle, which was probably metasomatized by slab-derived fluid/melt, while the northeastern group possibly formed by the mixing of an enriched lithospheric mantle melt and an depleted asthenospheric mantle melt. On the Fe_2O_3 vs. TiO_2 plot (Fig. 8A), the composition range of the Tongshankou MMEs mostly fall between the fields of experimental enriched and depleted peridotite melts, except for one sample plotted in the field of experimental enriched peridotite melt (the fields are after Falloon et al., 1988). The MMEs compositional fields also overlap with those of southwestern group of Cretaceous mafic rocks from the MLYRB. As can be seen on Nb/Th vs. Zr/Nb plots (Fig. 8B), most of the samples from the MMEs and the southwestern group of MLYRB Cretaceous mafic rocks plot in the field of the upper continental crust (UC) and enriched mantle (EM) (the fields are after Condie et al. (2002) and references therein). Therefore, these geochemical features of the Tongshankou MMEs suggest that they were most likely derived from enriched lithospheric mantle. Their relatively high Th/La values and Th contents with low Sm/La and U/Th values (Figs. 8E and F) further suggest that the isotopically enriched lithospheric mantle source has been metasomatized by the melt from subducted oceanic sediments (Ge et al., 2003). This possibility also is supported by the narrow Nd and relatively wide Sr isotopic values of the MMEs, which have a distinct trend pointing to an enriched mantle (EM II) (Fig. 9D). EMII is attributed to a mantle source that was metasomatized by subduction recycling of sediment (Chauvel et al., 1992; Zindler and Hart, 1986). This trend is very common in some examples which were suggested to have been derived from the enriched mantle (EMII), for example the MMEs in Dexing district and the basalts in the Society Islands (Hou et al., 2013; Hawkesworth et al., 1984). The Zircon T_{DM} ages of the MMEs varies from 1030 to 1223 Ma (Supplementary Table S4), implying that the metasomatism of mantle source is likely to be caused by ancient subduction before the collision of the Yangtze block and Cathaysia block at 970 Ma (Li and McCulloch, 1996).

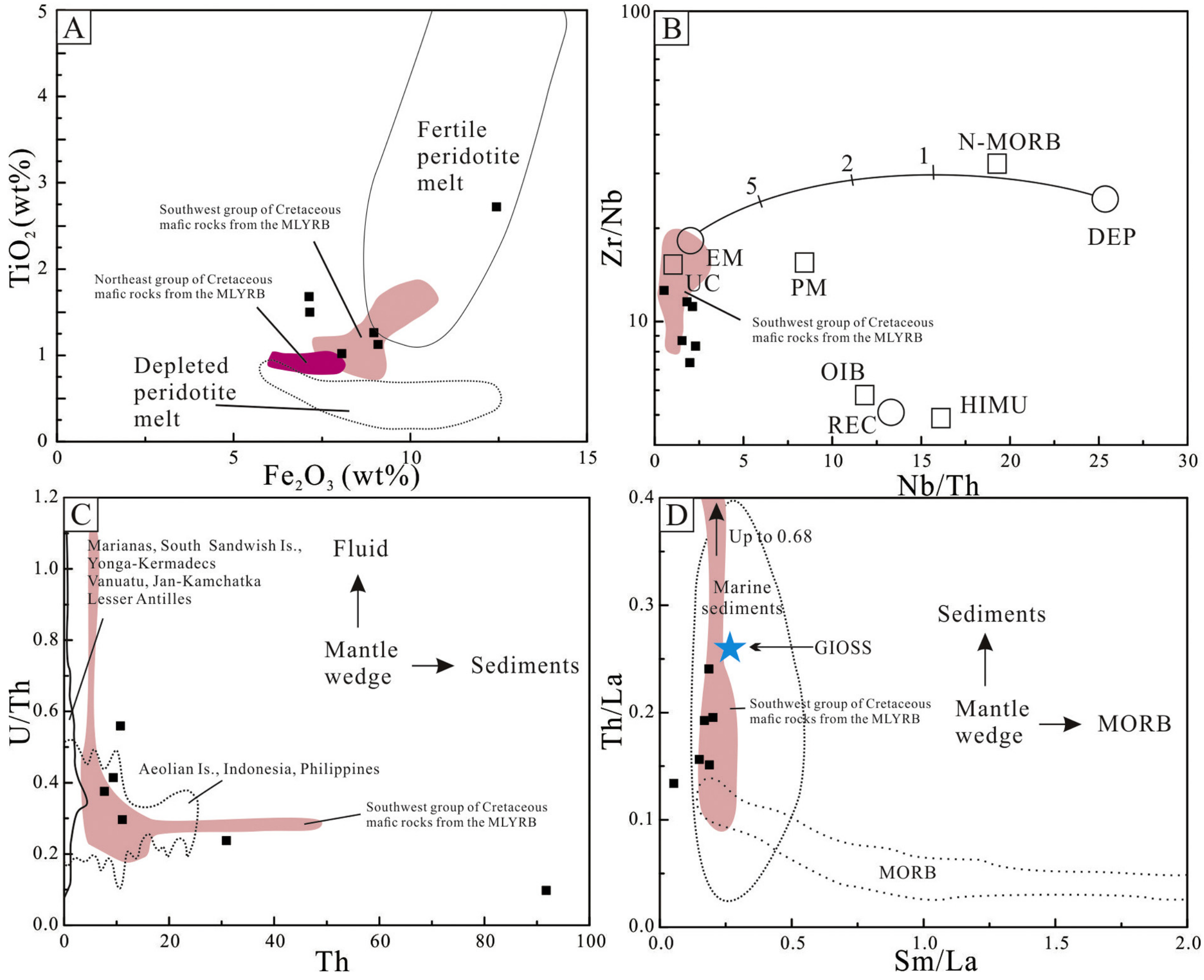

Fig. 8. (a) Petrological variations of MMEs. The data fields for the fertile and depleted peridotite melts are after Falloon et al., 1988; the northeast group and the southwest group of Cretaceous mafic rocks from the MLYRB are after Xie et al. (2006), Wang et al. (2006), Yan et al. (2008) and Yuan et al. (2008). (b) Zr/Nb versus Nb/Th diagrams for for the samples from Tongshankou deposit (Condie et al., 2002). The fields for DEP (depleted mantle), EM (enriched mantle), N-MORB (normal MORB), OIB (oceanic island basalts), PM (primitive mantle), REC (recycled slab component), and UC (upper continental crust) are after Condie et al. (2002) and references therein. (c) U/Th versus Th diagram (Hawkesworth et al., 1997). (d) Th/La versus Sm/La diagram (Plank, 2005). The field for MORB is after Plank (2005). The data for marine sediments and GLOSS (global subducted sediments) are from Plank and Langmuir (1998) and Xie et al. (2006).

5.2. Petrogenesis of Tongshankou granodiorite and quartz diorite porphyries

Tongshankou granodiorite and quartz diorite porphyries have high Sr (≥759 ppm; ≥943 ppm), low Yb (≤1.09 ppm; ≤1.17 ppm) and Y (≤12.6 ppm; ≤14.0 ppm) contents and relative high Sr/Y (71.1–74.4; 67.4–70.3) and $(La/Yb)_N$ (20.4–30.9; 29.5–33.4) values (Figs. 9A and B). These geochemical characteristics are similar to adakites which was first coined by Defant and Drummond (1990).

The origin of the rocks with adakite-like compositions in Tongshankou has been a subject of debate over the last decade, with models of (1) melting of delaminated lower crust in the lithospheric mantle (Wang et al., 2004), (2) large-scale melting of metasomatized mantle peridotite (Li et al., 2008), and (3) fractional crystallization processes of basaltic magmas from mantle peridotite (Li et al., 2013). These debates mainly focused on the magmatic process and the magma source of the mineralization-hosted Tongshankou granodiorite porphyry.

5.2.1. Magmatic processes of the porphyries: batch partial melting or fractional crystallization?

Li et al. (2013) proposed that fractional crystallization played a major role in the genesis of the ore-bearing and ore-barren rocks with adakitic signature in the MLYRB. This hypothesis is based on the decreasing trend in a log–log correlation plot between Sc and Rb, and also the decreasing contents of TiO_2, Fe_2O_3, MgO, CaO, P_2O_5 and Sc with increasing SiO_2. On the contrary, Li et al. (2008) and Wang et al. (2004) proposed that partial melting may play a dominant role in the magmatic evolution of Tongshankou granodiorite.

The negative correlations between MgO and SiO_2 (Fig. 7A), CaO/Al_2O_3 and SiO_2 (Fig. 10A) show that fractionation of clinopyroxene may have occurred in the magmatic process of the studied rocks. Amphibole fractionation may also have occurred, as reflected by the negative correlations between $Fe_2O_3^T$, MgO and SiO_2 (Figs. 7A, B), and between Dy/Yb with SiO_2 (Fig. 10B) (Davidson et al., 2007). Plagioclase fractionation may be insignificant, judging from major element variations and the negligible Eu anomalies of the rocks. These above mentioned correlations indicate that some fractional crystallization of clinopyroxene and/or amphibole do exist during the magmatic evolution of the studied rocks. But, these correlations do not apply to assessing the contribution of partial melting in the magmatic process. The correlations between C^H/C^M and C^M (M-magmatophile elements, i.e., REE, Zr, Hf; H-hypermagmatophile elements, i.e., Ta, Th, La, Ce; Treuil and Joron, 1975), the correlation between compatible (Sc, Cr, Ni) and incompatible (Rb, La, Th, U, Cs) trace elements (Cocherie, 1986), the correlation between different incompatible trace elements

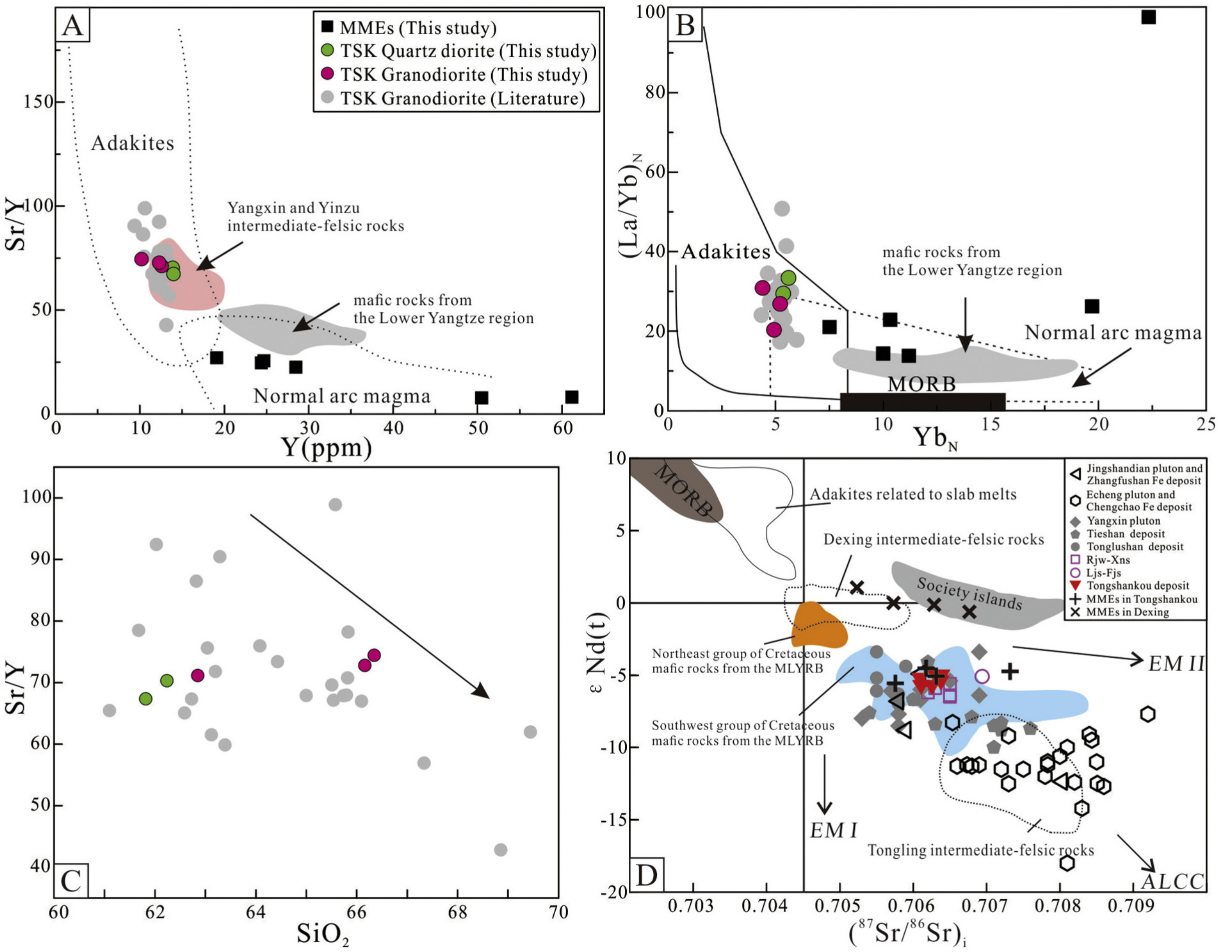

Fig. 9. Plots of Sr/Y versus Y (a) and $(La/Yb)_N$ versus Yb_N (b) for the samples from Tongshankou deposit. The adakites and Normal arc magma fields are from Defant and Drummond (1990). Yangxin and Yinzu intermediate-felsic rocks with adakitic signature (Wang et al., 2004). data fields for the mafic rocks from the Lower Yangtze region (Xie et al., 2006; Wang et al., 2006; Yan et al., 2008; Yuan et al., 2008). (c) Sr/Y versus SiO_2 diagram. (d) εNd(t) values Initialized $^{87}Sr/^{86}Sr$ ratios variation diagram for the samples from Tongshankou deposit together with Late Mesozoic mineralization-associated intrusions in the selected Cu—Fe and Fe skarn deposits of the Edong ore district, MLYRB, China. For comparison, also shown are the compositional fields of Tieshan, Echeng, Yangxin and Jinshandian plutons in the Edong ore district (Chen et al., 2001; Li et al., 2009; Wang et al., 2003; Xie et al., 2008; Zhao et al., 2010), data fields for the northeast group and the southwest group of Cretaceous mafic rocks from the MLYRB (Xie et al., 2006; Wang et al., 2006; Yan et al., 2008; Yuan et al., 2008), data fields for Tongling and Dexing intermediate-felsic rocks with adakitic signature (Wang et al., 2003; Hou et al., 2013, respectively), data fields for Society islands (Hawkesworth et al., 1984).

(Schiano et al., 2010) and the correlation between C^I versus C^I/C^C (where I is an incompatible element, such as H or M, and C a compatible element; Schiano et al., 2010) are four robust ways to assessing the contributions of partial melting and fractional crystallization in magmatic processes. As can be seen from Fig. 10D, the Tongshankou granodiorite and quartz diorite porphyries show a strong positive correlation in the La/Sm vs. La plots. Approximate linear correlations in Fig. 10E do not point towards the origin in the plots of highly incompatible elements, contrary to what is expected during fractional crystallization (the ratios between the concentrations of incompatible elements H1 and H2 may keep constant during fractional crystallization process and equal to their ratios in the source material, Schiano et al., 2010). The compatible trace element contents (e.g., Sc: 2.1–10.2 ppm) of the analyzed rocks slightly increase with a relatively increasing of incompatible trace elements (e.g., Rb: 60.5–183.61 ppm; Fig. 10F). Furthermore, the data lie on straight lines on the companion Rb versus Rb/V plot (Fig. 10G). These geochemical features indicate that batch partial melting played a significant role in the generation of the studied rocks.

5.2.2. Magma source of the porphyries and the origin of the "adakitic" signatures

Adakites are a rare but petrogenetically significant subduction related magma series as they provide strong evidence for melting of the basaltic oceanic crust during subduction (Danyushevsky et al., 2008; Defant and Drummond, 1990; Kelemen et al., 2003; Martin et al., 2005; Patriat et al., 2019). One of the most significant geochemical characteristics of adakites is their high Sr/Y values indicating the absence of plagioclase as a residual phase in melting process of a basaltic crustal source, however the absolute magnitude of the Sr/Y value which is used to define adakites varies in the scientific literature (e.g. ≥20

Fig. 10. (a–c) Harker diagrams of the Tongshankou porphyries. Plots of La/Sm versus La (d), Sc versus Rb (e), La versus Rb (f), and Rb versus Rb/V (g), the data for the samples from Tongshankou deposit s indicate that batch partial melting played a major role in the generation of studied rocks. (h) SiO_2 versus Mg# for the Tongshankou adakite compositions and MME determined in this study. Mg# is calculated on the basis of an $Fe^{2+}/(Fe^{2+}+Fe^{3+})$ value of 0.8 appropriate for an oxidised enriched mantle melting. The Juvenile Crustal and Enriched Mantle Melts are from the Supplementary Table S4. Note that a mixing line between the two model melts can explain the range in compositions from Tongshankou. As this is a simplified model we have ignored the role of crystal fractionation which has also been involved in the petrogenesis of the porphyry (see Text S2). The mixing model has the advantage of both explaining the linear major oxide trends, relatively high Mg#, and the metaluminous character of the Tongshankou porphyry (see Text S2 for discussion). HSA, LSA – refers to High Silica Adakite and Low Silica Adakite respectively (Martin et al., 2005; Danyushevsky et al., 2008) and HMA and LMA refer to High Magnesian and Low Magnesian Andesite respectively (Kelemen et al., 2003). The shaded rectangle delineates the range of Mg# which some authors (e.g. Rapp and Watson, 1995; Rapp et al., 2003) believe distinguish crustal melts (<40–45) from melts which have interacted with or produced within the mantle (>40–45).

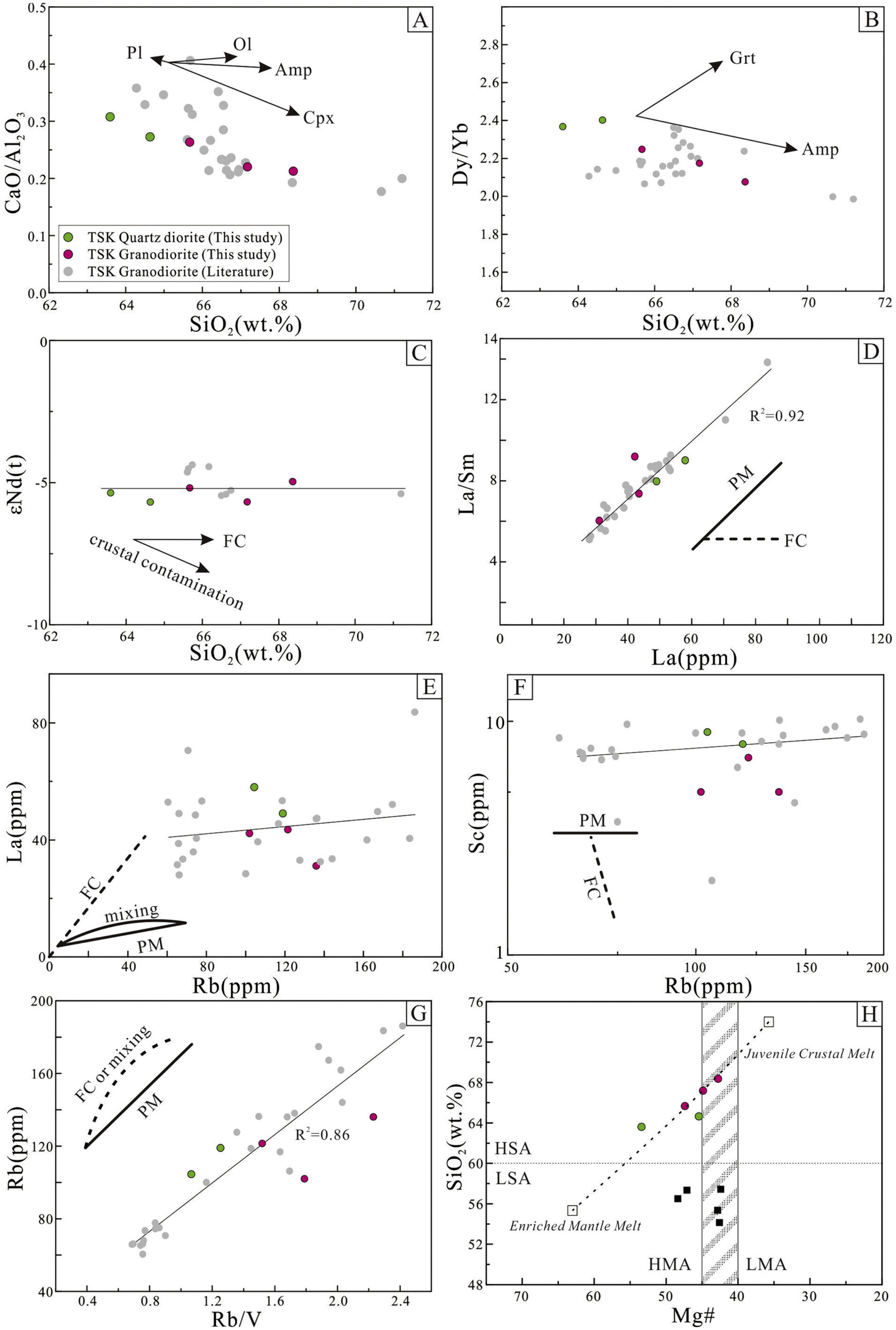
A
CaO/Al$_2$O$_3$
0.5
0.4
0.3
0.2
0.1
0.0
62
64
66
68
70
72
SiO$_2$(wt.%)
Pl
Ol
Amp
Cpx
● TSK Quartz diorite (This study)
● TSK Granodiorite (This study)
● TSK Granodiorite (Literature)
B
Dy/Yb
2.8
2.6
2.4
2.2
2.0
1.8
1.6
62
64
66
68
70
72
SiO$_2$(wt.%)
Grt
Amp
C
εNd(t)
0
-5
-10
62
64
66
68
70
72
SiO$_2$(wt.%)
FC
crustal contamination
D
La/Sm
14
12
8
4
0
20
40
60
80
100
120
La(ppm)
R^2=0.92
PM
FC
E
La(ppm)
80
40
0
0
40
80
120
160
200
Rb(ppm)
FC
mixing
PM
F
Sc(ppm)
10
1
50
100
150
200
Rb(ppm)
PM
FC
G
Rb(ppm)
200
160
120
80
40
0.4
0.8
1.2
1.6
2.0
2.4
Rb/V
FC or mixing
PM
R^2=0.86
H
SiO$_2$(wt.%)
76
72
68
64
60
56
52
48
70
60
50
40
30
20
Mg#
Juvenile Crustal Melt
Enriched Mantle Melt
HSA
LSA
HMA
LMA

Richards and Kerrich, 2007; >50 Kelemen et al., 2003) making it somewhat arbitrary the assignment of the name ‘adakite’ to any particular magmatic rock. Despite this lack of consensus, the high Sr/Y values (>67) of the Tongshankou quartz diorite and granodiorite clearly make them adakites.

This is confirmed by the very close agreement in major and trace element geochemistry between the Tongshankou quartz diorite and modern day adakites from active subduction zones in the SW Pacific (e.g. Southern Vanuatu, Patriat et al., 2019; Fiji, Danyushevsky et al., 2008). If we take this close correspondence in geochemistry with adakites erupted in modern subduction settings as signifying similar petrogenetic processes, such as slab melting and volatile-fluxed mantle melting above a subducting slab forming an arc volcanic front within ~100 km of the trench, we then have a serious difficulty with the petrogenesis of the Tongshankou adakites. Although there is an oceanic slab at great depth beneath Eastern China (proto-Pacific oceanic crust) the active volcanic front is currently located along the Izu-Bonin-Mariana subduction zone. For the Tongshankou adakties to have formed by slab melting they would have to have been located at a volcanic front at ~143-145 Ma – however geodynamic studies have demonstrated that the proto-Pacific oceanic plate subduction commenced at ~250 Ma (Liu et al., 2017). By the Early Cretaceous, the active volcanic front was located along the eastern side of the Central Range of Taiwan, ~1200 km to the east of the Edong intrusions (Zhou and Li, 2000). Thus at ~143-145 Ma the Edong district was situated within an extensional, continental back-arc setting (Yan et al., 2008).

However, the geochemistry of the MMEs and the Tongshankou adakites all have strong subduction zone trace element enrichments despite their location well away from any active volcanic front at the time of their formation. As shown in the Fig. 9D, The Sr—Nd isotopic compositions of all the studied rocks associated with the Tongshankou porphyry deposit exhibit extremely concordant isotopic compositions with an enriched isotopic signature. This characteristic is strikingly distinct from the ancient basement and the depleted mantle, but similar to the ore-bearing intrusions in the Edong district which are related to W-Cu-Mo deposits (Ruanjiawan-Xiniushan, Longjiaoshan-Fujiashan) and Cu-Fe-Au deposits (Tonglushan, Jiguanzui, Yangxin, Tieshan). The data also overlap some of the Early Cretaceous mafic volcanic rocks from the MLYRB, which have been proposed to be the magma directly derived from an enriched lithospheric mantle source (Wang et al., 2006; Yan et al., 2008). The most satisfactory explanation for this is that the subduction geochemical fingerprint has been inherited from a prior ancient subduction event which has formed a metasomatized enriched mantle - formerly the mantle wedge above a paleo-subduction event and was present as part of the lithosphere beneath South East China at 143–145 Ma (Li et al., 2008, 2009). This paleo-subduction event mostly likely occurred prior to and during the collision of the Cathysia and Yangzi cratons in south China at ~970 Ma (Li and McCulloch, 1996). This is consistent with zircon T_{DM} ages of the MMEs and the Tongshankou adakites which are 1199 to 915 Ma (Supplementary Table S4).

This enriched lithospheric mantle has subsequently melted due to the influx of hot upwelling asthenospheric mantle in response to the roll-back of the proto-Pacific slab, resulting in the ‘decratonization’ of South East China lithosphere. Indeed, the MMEs along with associated mafic volcanism of similar age in the MLYRB all have compositions consistent with high-K to shoshonitic magmatic suites (Fig. 4B). This is significant as shoshonitic suites, in general, do not seem to be directly related in time and space to active subduction. They commonly occur in environments presently far away from active sites of subduction. Extension transtensional tectonics can remobilize older subduction modified sources resulting in magmas with arc-like geochemical characteristics, long after subduction has ceased. They are also considered to be associated with the convective thinning of the lithosphere (Turner et al., 1996; Leslie et al., 2009).

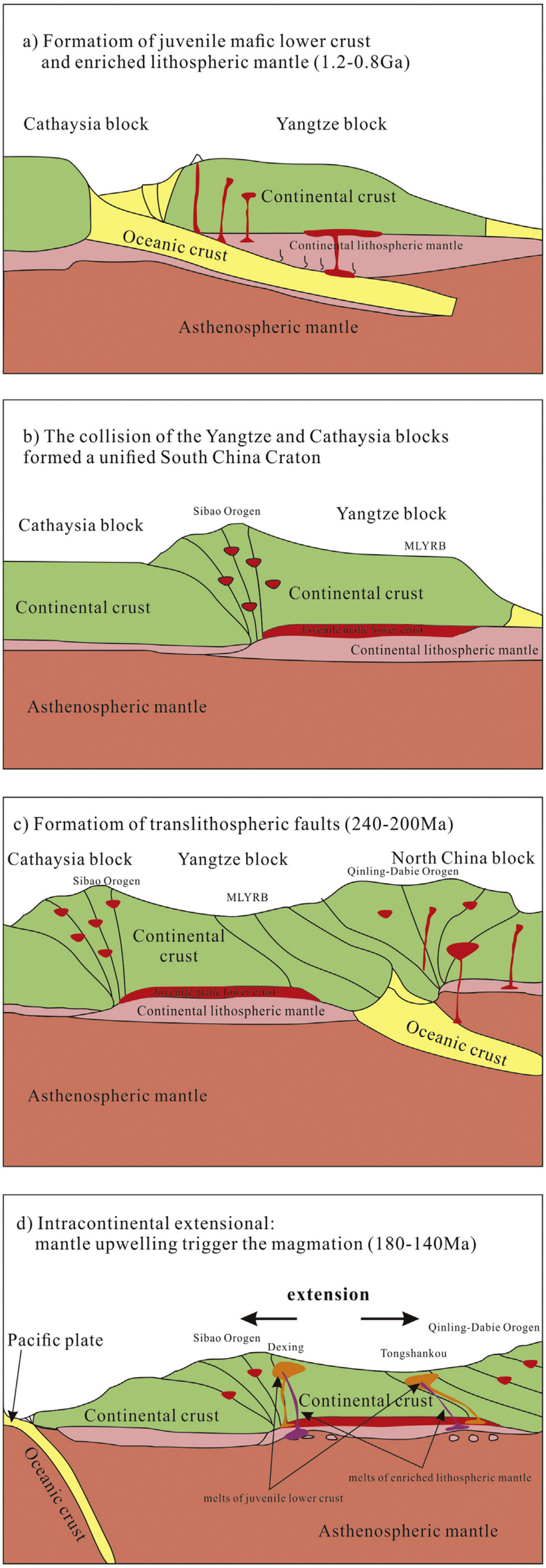

Fig. 11. A sketch plot showing the generation of Tongshankou porphyry system.

Although the origin of the Tongshankou MME can be reasonably related to melting of an enrichment mantle source this leaves us with a major question - is the adakitic signature of the Tongshankou intrusion also inherited from the same enriched mantle or is it inherited from a crustal source? The geochemistry of the Tongshankou adakites have several features which makes it very unlikely for it to be produced either by melting of an enriched mantle source or melting of a crustal source alone, as outlined below;

5.2.2.1. Melting of single enriched mantle source?. Li et al. (2008) proposed large-scale partial melting of enriched lithospheric mantle can directly generate the ore forming magma of Tongshankou deposit. This hypothesis was mainly based on the assumption that slab melts equilibrated with mantle peridotite will transfer their adakitic signature to the magmas derived from such a metaosmatizd mantle (Kay, 1978; Yogodzinski et al., 1994, 1995). However, the adakitic rocks derived from this process should have low SiO_2 (rarely above 60%), high MgO (usually above 3%), high Ni (average 103 ppm), high Cr (average 157 ppm), and high Sr (mostly above 1000 ppm) contents due to interaction between basaltic melt and peridotite (Martin et al., 2005). Instead, Tongshankou granodiorite and quartz diorite have high SiO_2 (average 63.9%), low MgO (average 1.9%), Ni (average 11 ppm), Cr (average 23 ppm) and low Sr contents (average 894 ppm) corresponding to the geochemical characteristics of high-silica adakites described by Martin et al. (2005). Most researchers agree that tonalites (and quartz gabbros) saturated with quartz and with Mg# ratios of 40 to 50 cannot be derived directly from peridotite (i.e., Green, 1973; Gromet and Silver, 1987).

Li et al. (2009) recognizing these difficulties proposed that the parental magmas for the adakitic ore-related rocks were primitive high-MgO low-silica adakitic parents produced by melting of adakitic metasomes in the enriched mantle lithosphere. The high-silica adakitic ore-related rocks were derived from these adakitic parental melts by extensive crystal fractionation, dominated by olivine at mantle depth (about 50 wt%, Li et al., 2009). Although this model can satisfactorily explain the major and trace element geochemical characteristics of Tongshankou adakites, it suffers from two significant weaknesses: Firstly, based on our knowledge of adakites erupted in well-defined Neogene-Recent subduction settings, adakitic magmas always have depleted Sr and Nd isotopic values similar to the subducting MORB crust – and is one of the key features identifying their origin as a result of slab melting. Associated arc magmas in general have low εNd(t) values and high $^{87}Sr/^{86}Sr$ values reflecting greater inputs from subduction derived fluids or sediment melts. For example, adakites from Kadavu Island in Fiji have εNd(t) values as high as 7.84 and $^{87}Sr/^{86}Sr$ values as low as 0.70296, whereas coeval subduction related volcanism have εNd(t) values < 6.5 and $^{87}Sr/^{86}Sr > 0.70405$ (Danyushevsky et al., 2008; Leslie et al., 2009); and secondly, there is currently no evidence in the Edong district of primitive rocks or cumulates which are associated with the earlier stages of fractionation proposed by Li et al. (2009).

Li et al. (2013) however, have argued that the ore-bearing rocks in MLYRB, including Tongshankou, were generated by fractional crystallization of basaltic magma as opposed to an adakitic parental magma. Li et al. (2013) proposed that fractional crystallization of ~17.2% hornblende, ~5.7% magnetite and ~0.1% titanite from the melts resulted in the evolved basaltic andesitic melts with “adakitic” geochemical features of the ore-bearing porphyries. However, the fractional crystallization model proposed by Li et al. (2009) and Li et al. (2013) are based on a prerequisite, i.e., the studied rocks are derived from a same source with a similar magmatic evolution process. But there are risks in arbitrarily asserting the existence of this premise and drawing such conclusions from just one diagram (see discussion in Section 5.2.1). As mentioned above, the geochemical features indicate that batch partial melting has played a major role in the magma process of Tongshankou porphyries, even though some evidence of fractional crystallization is apparent in the formation of the studied rocks. Furthermore, if the “adakitic” signatures of the Tongshankou adakitic rocks were generated mainly by fractional crystallization of basaltic magma, it will show a significant positive correlation between the Sr/Y ratio and SiO_2, whereas the correlation in Tongshankou porphyries is reversed (Fig. 9C). In addition, basaltic magmas derived from mantle peridotite always have high content of MgO, Cr, Ni and low SiO_2. It therefore requires a significant amount of fractional crystallization involving amphibole and other ultramafic minerals to produce intermediate-felsic magma. However, fractional crystallization of amphibole not garnet requires that the magma stayed in the deep level of continental lower crust (about 30–40 km) for a long time which would result in large-scale assimilation and mixing between the magma and the wall rocks. This is inconsistent with the Sr-O-Nd isotopic signatures in the MLYRB adakitic rocks which clearly show crustal contamination only played little role in their magma process (Fig. 10C; Li et al., 2013). In general, models which invoke high-pressure crystallization from normal arc basaltic magmas ignore the fact that garnet is a late crystallizing phase (Müntener and Ulmer, 2006) and subsequently only modest increases in Sr/Y values are possible. As well these models also ignore the fact that evolved melts in equilibrium with garnet are corundum normative – unlike any adakitic magma (see supplementary discussion in Danyushevsky et al., 2008).

5.2.2.2. Melting of single crustal source?. Another viable alternative possibility for the origin of the Tongshankou adakites is melting of a thickened juvenile lower crust which has been proposed to explain the presence of high SiO_2 adakitic magmas in a variety of subduction settings (Atherton and Petford, 1993; Hou et al., 2004; Richards and Kerrich, 2007). However, there is no evidence for thickened crust beneath the LYRMB – which is currently only approximately 30–31 km thick (Zhai et al., 1992) and it is very unlikely that extensive delamination of >40 km of crust has occurred since the Early Cretaceous (Ma et al., 2019). As well, there is to date, no evidence of any outcropping lower crustal eclogite or garnet-bearing assemblages beneath the eastern Yangtze craton nor is there any evidence for garnet-bearing crustal xenoliths entrained in Cretaceous basalts (Li et al., 2009).

Added to this complete lack of thickened or delaminated crust in the Edong area, the Tongshankou adakites are unlike any crustal melt with regards to their metaluminous nature and high Mg# values. The melting of lower crustal source rocks (e.g. eclogite, amphibolite eclogite or amphibolite) will produce low Mg# melts (<45–40; Rapp et al., 2003; Rapp and Watson, 1995; Richards and Kerrich, 2007; Qian and Hermann, 2013), whereas the Tongshankou adakites extend to high Mg# values (Fig. 10H; high Mg# is defined by Kelemen et al., 2003 as Mg# values >50). As well, most of the experimental melting studies of crustal source rocks produce peraluminous compositions (e.g. Qian and Hermann, 2013).

However these features of the Tongshankou adakites could potentially be explained by reaction of a crustal melt within the mantle to produce high Mg# (Kelemen, 1995, Kelemen et al., 1998). A potential proposed mechanism for this is crustal delamination into hot mantle. For example, Wang et al. (2004) proposed a model of crustal delamination, which the underlying lithospheric mantle imparts its enriched isotopic signature to the crustal melt produce from the delaminated crust. Further the presence of garnet in the mantle as a residual phase depletes the reacting crustal melt in Y and Yb at depths (>40 km) with the lithospheric mantle. There are however several difficulties with a crustal delamination as an explanation for the high Mg# and metaluminous nature of the Tongshankou adakites: delamination of ancient lower crust requires the rocks to metamorphose into garnet-rich amphibolites and/or eclogite facies rocks (Kay and Kay, 1993). As a result, $(Gd/Yb)_N$ values can be used as an important fingerprint of residual garnet during melting at depth (>5.8; Huang and He, 2010). In the Dabie orogeny, the Fuziling intrusion which has been proposed to be the result of partial melting of the mafic lower crust controlled by garnet at high pressure has high $(Gd/Yb)_N$ up to 9.5 (Wang et al., 2007). However, the

Tongshankou granodiorite and quartz diorite have relatively low $(Gd/Yb)_N$ values (2.6–3.1). The Dy/Yb-SiO_2 diagram (Fig. 10B) also shows that the Tongshankou adakies have small decreases in Dy/Yb values with relative increase in SiO_2 suggesting some degree of amphibole as a crystallizing or residual phase. This geochemical characteristic is quite different with typical adakites formed by partial melting of delaminated lower crust which usually shows garnet control (Gao et al., 2004). So, we consider crustal melting or delamination of crust in the lithospheric mantle as an unlikely mechanism for producing the Tongshankou adakites.

5.2.2.3. Mixing of melts from juvenile lower crust and enriched mantle lithosphere. In view of the above difficulties we propose a petrogenetic model which accounts for the formation of Tongshankou porphyries. As mentioned above, the major and trace element characteristics of Tongshankou granodiorites and quartz diorites indicate that batch partial melting played a significant role in the generation of studied rocks. Since the mantle peridotite cannot be the direct source of the high-silica Tongshankou felsic porphyries, there must be a source at shallow depth in the crust (<40 km), which has enriched isotopic signature and also the ability to generate "adakitic" magma. In recent years, more and more researchers have found that the formation of the "adakitic" signature is depended on two aspects: (i) the enrichment of Sr/Y and La/Yb during partial melting. Under appropriate pressures, crustal melts can become 10–20 times more enriched in incompatible element ratio values over their source, due to the stability of garnet and other phases (Moyen, 2009); (ii) the Sr/Y and $(La/Yb)_N$ values of the original crustal source will have a significant influence on the resulting values in the subsequent crustal melt (Jiang et al., 2007; Moyen, 2009). Therefore, if we have a source with high initial Sr/Y and $(La/Yb)_N$ values, the magma source of adakitic rocks can be much shallower, and does not necessarily require the presence of garnet (Qian and Hermann, 2013). In the study of Jurassic adakitic rocks in the northern part of the North China Craton, Ma et al. (2015) further highlighted that the "adakitic" signature of rocks may be inherited from their source rocks during partial melting. We therefore propose that the Tongshankou granodiortie and quartz diorite were most likely formed by dehydration melting of juvenile mafic lower crust which was dominated by amphibolite with "adakitic" signature. Nonetheless, the challenge is how could such special lithological unit form during orogenesis?

In the subduction zone, Carmichael (2002) suggested that only ~20% of the total arc magma is actually erupted at the surface as volcanic rocks, the rest crystallizes at depth as hornblende gabbros and cumulates (Anderson Jr., 1980; Takahashi et al., 2005). Partial melting of the lower crust is likely to be triggered by intrusion of hot and mantle-derived mafic magmas followed by fractionation and intermixing (i.e., Eichelberger, 1978; Hildreth, 1981; Fyfe, 1992; Snyder and Tait, 1998; Dufek and Bergantz, 2005). During the assimilation and homogenization between the melts of the mantle and lower crust, the mixing ponded basaltic magma loses heat to the crust, resulting in fractional crystallization leaving a cumulate residue of mafic silicates potentially including garnet, pyroxenes, and amphibole (Claeson and Meurer, 2004; Müntener and Ulmer, 2006). The resultant mafic cumulates will be of high density and, although formed at the base of the crust, would be identified seismically as mantle, with the top of the ultramafic cumulate zone representing the Moho (Hamilton, 1981; Griffin and O'Reilly, 1987; Müntener et al., 2001). If there is limited crustal assimilation during the formation of the underplated juvenile crust, the Sr—Nd isotopic values of the juvenile mafic lower crust will be identical to the underlying metasomatized mantle, as both are formed during the same paleo-subduction event. Similar models have been invoked to explain the genesis of granitoids and volcanic rocks with adakitic geochemical signatures in continental arcs (i.e., Feeley and Hacker, 1995; Tulloch and Kimbrough, 2003) and intercontinental extensional settings (i.e., Hou et al., 2013).

Considering the geochemical characteristics of the adakitic rocks and the MMEs in Tongshankou deposit, we think that the formation of the studied rocks cannot be explained by a single enriched mantle source or a single crustal source.

The suitable model to explain the adakitic nature of the Tongshankou magmas is the mixing of a crustal melt derived by melting of an amphibolite bearing juvenile lower crust and a mantle melt derived from melting of enriched lithospheric mantle. Both melts are the result of the upwelling of asthenospheric mantle in response to proto-Pacific slab roll-back and back-arc transtensional extension and rifting. The juvenile crust is capable of producing high Sr/Y values due to both i) inheritance from the original composition of the bulk juvenile crust and ii) enrichment due to melting. However the high $(La/Yb)_N$ and Mg# values, along with the metaluminous nature of the Tongshankou magams are the result of mixing with a melt derived from the enriched mantle lithosphere. This mixing also gives a good explanation for the linear trends in major element and trace element ratio values previously discussed above (Fig. 10H). In the Supplementary Table S5 and Fig. 10H we outline a simple model mixing calculation which demonstrates how our proposed juvenile crust-enriched mantle hybridization model can explain the geochemistry of the Tongshankou adakites.

The Tongshankou MMEs represent evolved melts produced during the initial stages of decratonization due to upwelling of hot asthenospheric mantle and vigorous mantle convection, which was caused by the subduction of paleo-Pacific plate and the subsequent intracontinental extension during the Late Mesozoic (Xu, 2001; Zheng et al., 2015). Based on petrological and experimental studies of high-K and shoshonitic suites (Foley, 1992; Turner et al., 1996; Leslie et al., 2009) the MME parental melts were likely to have been absarokitic in nature and produced <5% melting of a veined metasomatized mantle (veins of cpx and mica ± apatite and carbonate, Foley, 1992). As the decratonization process developed, melting occurred at shallower depths due to the continued upwelling of hot asthenospheric mantle. Eventually the juvenile lower crust begins to melt and mix with melts produced at a shallower level within the enriched metasomatized mantle. The earlier produced magmas were incorporated as MME within the Tongshankou adakitic magma. Thus although the MME are related to the same overall geodynamic process and are essentially coeval in space and time, they are not parental or are involved in mixing with juvenile crustal derived melts.

6. Geodynamic implications for the MLYRB

The Late Jurassic to Early Cretaceous tectonic–magmatic evolution of the MLYRB has long been the focus of controversy. There are three distinct models have been proposed, i.e., oceanic ridge subduction (Ling et al., 2009; Sun et al., 2010), flat subduction (Li and Li, 2007; Li et al., 2013), and intracontinental extension (Chang et al., 1991; Wang et al., 2006; Zhou et al., 2015).

The traditional continental magmatic arc can't explain the ca. 1300 km width of the magmatic province, the presence of A-type granites and the absence of a large amount of andesite. Li and Li (2007) proposed a flat subduction model, which not only explained the broad intracontinental orogeny, but also explained the presence of a vast fault basin above the orogeny. Li et al. (2013) further suggested the foundering of flat slab can interpret the near-concentric circular spatial and temporal distribution of the magmatism in eastern South China during the Jurassic and Cretaceous. But there are two huge orogenic belts (Qinling-Dabie orogenic belt and Sibao orogenic belt) near the MLYRB which have thick lithosphere. The subduction angle of the oceanic crust could be severely limited by the great thickness of rigid lithosphere. Moreover, both of the two models suggest that the adakitic rocks in MLYRB were formed by fractional crystallization of mantle derived basaltic magma. This is inconsistent with the isotopic and geochemical characteristics of the Tongshankou porphyries.

Oceanic ridge subduction model proposed by Ling et al. (2009) and Sun et al. (2010), mainly based on the presence of A-type granitoids, and Nb-enriched basalts. However none of these two types of rocks are coeval with the generation of the studied rocks (~143 Ma). In this model, partial melting of subducting young and hot oceanic slabs close to the ridge was proposed for the formation of adakitic rocks. The negative εNd(t) values of adakitic rocks were plausibly explained by magma mixing between adakitic magmas and enriched lithospheric mantle melt, and/or crustal materials through AFC process. But, the isotopic characteristics of Tongshankou porphyries indicate that source contamination, rather than crustal contamination, played a major role in the generation of these adakite. Moreover, the high SiO_2 (average 63.9%), low MgO (average 1.9%), low Ni (average 11 ppm), low Cr (average 23 ppm) and low Sr contents (average 894 ppm) of Tongshankou porphyries are inconsistent with the adakitic rocks derived from this process, which should have low SiO_2 and high MgO (and also Ni, Cr and Sr) contents.

New evidence from the Tongshankou deposit, especially the contemporary MMEs, combined with the data of previous studies in the Edong district, gives us new constraints about the tectonic evolution and geodynamic background for genesis of Tongshankou porphyries and associated Cu-Mo-W mineralization. The geochemistry of the Tongshankou MMEs provides evidence for the nature of contemporary mantle-derived magmas. Based on the composition comparison between the ore-forming pluton and the MMEs, it is reasonable to believe that ore-forming rocks did not directly originate from the enriched mantle source like the MMEs. A juvenile mafic lower crust should have existed and served as the source of Tongshankou ore-forming porphyries. The existence of the juvenile mafic lower crust was also identified in the giant Dexing porphyry Cu deposit area and played an important role in the formation of the ore-forming rocks in Dexing (Hou et al., 2013). We further proposed that this juvenile mafic lower crust was formed in the late Mesoproterozoic era, during the subduction and collision between the Cathaysia and Yangtze blocks, based on the zircon T_{DM} ages of 1199 to 915 Ma (Supplementary Table S4). The zircon T_{DM} ages of the MMEs has similar range with their host rocks, thus the enriched characteristics of the mantle source of MMEs may also have formed at the same time.

Although we cannot completely rule out the contribution of material from the subduction of the paleo-Pacific plate, our results tell us that force and heat are sufficient. Therefore, we propose a geodynamic model, with the following three stages, for the generation of the Tongshankou MMEs, adakitic granodiortie and quartz diorite porphyries and related igneous rocks in this area. First, in the late-Mesoproterozoic, before the collision of the Cathaysia and Yangtze blocks at ca. 970 Ma (Li and McCulloch, 1996), the subduction process generated an enriched lithospheric mantle through the subducted oceanic sediments metasomatism. The hydrous basaltic magma derived from this mantle source intensively underplated beneath the lower continental crust and generated a juvenile lower crust which was dominated by amphibolite (Fig. 11A). The subsequent collision of the Cathaysia and Yangtze blocks formed a unified South China Craton (SCC; Fig. 11B). Secondly, in the Early Mesozoic, affected by the collision between the South China Craton and the North China Craton, trans-lithospheric faults in the MLYRB were extensively formed, such as the Xiangfan-Guangji and Tancheng-Lujiang faults, which provided pathways for upwelling magma (Fig. 11C). Finally, in the Early Cretaceous, since there is no direct evidence that the subduction of the paleo-Pacific plate must be the direct source of regional magma, we propose that the subduction may only provide the driving force for regional magmatism. Due to the oblique subduction of the paleo-Pacific plate towards the Eurasia plate and the reactivity of the trans-lithospheric faults, the MLYRB experienced extension of the lithosphere. This process caused asthenospheric mantle upwelling, providing additional heat to trigger the melting of both the juvenile mafic lower crust and enriched lithospheric mantle peridotite. Melting of enriched lithospheric mantle peridotite produced the parental magmas for the MMEs, meanwhile melting of juvenile mafic lower crust formed the parental magmas for the Tongshankou porphyries. These two different melts may have mixing at shallow crust and formed the Tongshankou porphyry system (Fig. 11D).

7. Conclusions

1. The granodiorite and the quartz diorite in Tongshankou Cu-Mo-W deposit is dated at 143.9 ± 0.6 Ma and 143.6 ± 0.7 Ma, respectively. The MMEs in both of the two prophyries is dated at 145.4 ± 1.9 Ma. Within the errors range permitting, the diagenesis ages of the enclaves is in agreement with their host rocks, both formed in earliest Cretaceous.
2. The granodiorite and the quartz diorite are geochemically similar to slab-derived adakites. Geochemical compositions, zircon ages and Nd–Sr–Hf isotope data indicate that they were most likely generated by mixing between a crustal melt derived from melting of an amphibolite bearing juvenile lower crust with adakitic signature and a mantle melt formed from melting of enriched lithospheric mantle.
3. The Tongshankou MMEs hosted in the ore-forming porphyries were most likely generated by magma mixing process. The petrography and geochemistry of the MMEs indicate that they were probably derived from an enriched mantle metasomatized by Proterozoic subducted oceanic sediments. Injection of such magmas into the lower crust-derived felsic magmas form the MMEs in the Tongshankou porphyry system.
4. The melting of juvenile mafic lower crust and enriched lithospheric mantle may be caused by the upwelling of asthenosphere mantle and the reactivity of the translithospheric faults in the intracontinental extensional environment.

Supplementary data to this article can be found online at https://doi.org/10.1016/j.gr.2020.02.004.

Funding

This work was supported by the Chinese academy of sciences strategic pilot science and technology special (XDB18000000), the National Natural Science Foundation of China (NSFC Projects 41725009), and the Special Public Welfare Scientific Research fund Project by Ministry of Land and Resources of the People's Republic of China (201511035).

CRediT authorship contribution statement

Gaobin Chu: Writing - original draft, Conceptualization, Validation. **Huayong Chen:** Conceptualization, Validation, Resources, Writing - review & editing, Project administration, Funding acquisition. **Trevor.J. Falloon:** Conceptualization, Validation, Writing - review & editing. **Jinsheng Han:** Methodology. **Shitao Zhang:** Formal analysis. **Jiamin Cheng:** Software. **Xiaobo Zhang:** Investigation.

Declaration of competing interest

The authors declare that they have no known competing financial interests or personal relationships that could have appeared to influence the work reported in this paper.

Acknowledgements

We appreciate the assistance of Siquan Sun and Yijun Zhao from Wuhan Institute of Geology and Mineral Resources, as well as Shanggang Jin and Zeming Li from the First Geological Team of Hubei Geological Bureau for their kind help during field work. And we also appreciate the help of Liang Li (Nanjing FocuMS Technology Co. Ltd.) for zircon age and isotopic analyses. Our data are available from authors.

References

Ames, L., Zhou, G.Z., Xiong, B.C., 1996. Geochronology and isotopic character of ultrahigh-pressure metamorphism with implications for collision of the Sino-Korean and Yangtze cratons, central China. Tectonics 15, 472–489.

Anderson Jr., A.T., 1980. Significance of hornblende in calc-alkaline andesites and basalts. Am. Mineral. 65, 837–851.

Atherton, M.P., Petford, N., 1993. Generation of sodium-rich magmas from newly underplated basaltic crust. Nature 362, 144–146.

Bacon, C.R., 1986. Magmatic inclusions in silicic and intermediate rocks. J. Geophys. Res. 81, 6091–6112.

Blundy, J.D., Sparks, R.S.J., 1992. Petrogenesis of mafic inclusions in granitoids of the Adamello Massif, Italy. J. Petrol. 33 (5), 1039–1104.

Boynton, W.V., 1984. Cosmochemistry of the earth elements: meteorite studies. In: Henderson, R. (Ed.), Rare Earth Element Geochemistry, Developments in Geochemistry, 2. Elservier, Amsterdam, pp. 89–92.

Carmichael, I.S.E., 2002. The andesite aqueduct: Perspectives on the evolution of intermediate magmatism in west-central (105–99°W) Mexico. Contrib. Mineral. Petrol. 143, 641–663.

Chang, Y.F., Liu, X.P., Wu, C.Y., 1991. The Copper–Iron Belt of the Lower and Middle Reaches of the Changjiang River. Geological Publishing House, Beijing 234.

Chappell, B.W., White, A.J.R., 1992. I- and S-type granites in the Lachlan Fold Belt. Trans. R. Soc. Edinb. Earth Sci. 83, 1–26.

Chappell, B.W., White, A.J.R., Wyborn, D., 1987. The importance of residual source material (restite) in granite petrogenesis. J. Petrol. 28, 1111–1138.

Chauvel, C., Hofmann, A.W., Vidal, P., 1992. HIMU-EM: the French Polynesian connection. Earth Planet. Sci. Lett. 110 (1–4), 99–119.

Chen, Z.H., Xing, G.F., 2016. Geochemical and zircon U–Pb–Hf–O isotopic evidence for a coherent Paleoproterozoic basement beneath the Yangtze Block, South China. Precambrian Res. 279, 81–90.

Chen, J.F., Yan, J., Xie, Z., Xu, X., Xing, F., 2001. Nd and Sr isotopic compositions of igneous rocks from the lower Yangtze region in eastern China: Constraints on sources. Phys. Chem. Earth Solid Earth Geod. 26, 719–731.

Claeson, D.T., Meurer, W.P., 2004. Fractional crystallization of hydrous basaltic arc-type magmas and the formation of amphibole-bearing gabbroic cumulates. Contrib. Mineral. Petrol. 147, 288–304.

Cocherie, A., 1986. Systematic use of trace-element distribution patterns in log–log diagrams for plutonic suites. Geochim. Cosmochim. Acta 50, 2517–2522.

Condie, K.C., Frey, B.A., Kerrich, R., 2002. The 1.75 Ga Iron King Volcanics in westcentral Arizona: a remnant of an accreted oceanic plateau derived from a mantle plume with a deep depleted component. Lithos 64, 49–62.

Danyushevsky, L.V., Falloon, T.J., Crawford, A.J., Sofia, A.T., Leslie, R.L., Verbeeten, A., 2008. High-Mg adakites from Kadavu Island Group, Fiji, southwest Pacific: evidence for the mantle origin of adakite parental melts. Geology 36 (6), 499–502.

Davidson, J., Turner, S., Handley, H., Macpherson, C., Dosseto, A., 2007. Amphibole "sponge" in arc crust? Geology 35 (9), 787–790.

Defant, M.J., Drummond, M.S., 1990. Derivation of some modern arc magmas by melting of young subducted lithosphere. Nature 347, 662–665.

Ding, L.X., Huang, G.C., Xia, J.L., 2014. Petrogenesis of the Longjiaoshan-Fujiashan porphyritic intrusion in Southeastern Hubei Province and implications for Cu-W mineralization. Acta Geol. Sin. 88 (8), 1513–1527 (in Chinese).

Dodge, F.C.W., Kistler, R.W., 1990. Some additional observations on inclusions in the Granitic Rocks of the Sierra Nevada. J. Geophys. Res. 95, 17841–17848.

Du, Y.S., Li, S.T., Cao, Y., Qin, X.L., Lou, Y.E., 2007. AFC-related origin of the Late Jurassic to Early Cretaceous intrusions in the Tongguanshan Ore Field, Tongling, Anhui Province, East China. Geoscience 21, 71–77.

Dufek, J., Bergantz, G.W., 2005. Lower crustal magma genesis and preservation: a stochastic framework for the evaluation of basalt-crust interaction. J. Petrol. 46, 2167–2195.

Eichelberger, J.C., 1978. Andesites in island arcs and continental margins: relationship to crustal evolution. Bull. Volcanol. 41, 480–500.

Falloon, T.J., Green, D.H., Hatton, C.J., Harris, K.L., 1988. Anhydrous partial melting of a fertile and depleted peridotite from 2 to 30 kb and application to basalt petrogenesis. J. Petrol. 29, 1257–1282.

Feeley, T.C., Hacker, M.D., 1995. Intracrustal derivation of Na-rich andesitic and dacitic magmas: an example from Volcán Ollagüe, Andean Central volcanic zone. The Journal of Geology 103, 213–225.

Foley, S., 1992. Vein-plus-wall-rock melting mechanisms in the lithosphere and the origin of potassic alkaline magmas. Lithos 28 (3–6), 435–453.

Frost, T.P., Mahood, G.A., 1987. Field, chemical, and physical constraints on mafic-felsic magma interaction in the Lamarck Granodiorite, Sierra Nevada, California. Geol. Soc. Am. Bull. 99 (2), 272–291.

Fu, L.B., Wei, J.H., Tan, J., Santosh, M., Zhang, D.H., Chen, J.J., Li, Y.J., Zhao, S.Q., Peng, L.N., 2016. Magma mixing in the Kalaqin core complex, northern North China Craton: linking deep lithospheric destruction and shallow extension. Lithos 260, 390–412.

Fyfe, W.S., 1992. Magma underplating of continental crust. Journal Volcanology and Geothermal Research 50, 33–40.

Gao, S., Ling, W.L., Qiu, Y.M., Lian, Z., Hartmann, G., Simon, K., 1999. Contrasting geochemical and Sm–Nd isotopic compositions of Archean metasediments from the Kongling high-grade terrain of the Yangtze craton: evidence for Cratonic evolution and redistribution of REE during crustal anatexis. Geochim. Cosmochim. Acta 63, 2071–2088.

Gao, S., Rudnick, R.L., Yuan, H.L., Liu, X.M., Liu, Y.S., Xu, W.L., Ling, W.L., Ayers, J., Wang, X.C., Wang, Q.H., 2004. Recycling lower continental crust in the North China craton. Nature 432, 892–897.

Gao, S., Yang, J., Zhou, L., Li, M., Hu, Z.C., Guo, J.L., Yuan, H.L., Gong, H.J., Xiao, G.Q., Wei, J.Q., 2011. Age and growth of the Archean Kongling terrain, South China, with emphasis on 3.3 Ga granitoid gneisses. Am. J. Sci. 311, 153–182.

Ge, X.Y., Li, X.H., Zhou, H.W., 2003. Geochronologic, geochemistry and Sr–Nd istopes of the Late Cretaceous mafic dike swarms in southern Hainan Island. Geochimica 32 (1), 11–20.

Green, D.H., 1973. Experimental melting studies on a model upper mantle composition at high pressures under water-saturated and water-undersaturated conditions. Earth Planet. Sci. Lett. 19, 37–53.

Griffin, W.L., O'Reilly, S.Y., 1987. Is the continental Moho the crustmantle boundary? Geology 15, 241–244.

Gromet, L.P., Silver, L.T., 1987. REE Variations Across the Peninsular Ranges Batholith: Implications for Batholithic Petrogenesis and Crustal Growth in Magmatic Arcs. Geochim. Cosmochim. Acta 28, 75–125.

Hamilton, W.B., 1981. Crustal evolution by arc magmatism. Phil. Trans. R. Soc. London 301, 279–291.

Hawkesworth, C.J., Rogers, N.W., van Calsteren, P.W.C., Menzies, M.A., 1984. Mantle enrichment processes. Nature 311, 331–335.

Hawkesworth, C.J., Turner, S.P., Mcdermott, F., Peate, D.W., van Calsteren, P., 1997. U–Th isotopes in arc magmas: implications for element transfer from subducted crust. Science 276, 551–555.

Hildreth, W., 1981. Gradients in silicic magma chambers: implications for lithospheric magmatism. J. Geophys. Res. 86, 10153–10192.

Holden, P., Halliday, A.N., Stephens, W.E., 1987. Neodymium and strontium isotope content of microdiorite enclaves points to mantle input to granitoid production. Nature 330 (6143), 53–56.

Hoskin, P.W., Schaltegger, U., 2003. The composition of zircon and igneous and metamorphic petrogenesis. Rev. Mineral. Geochem. 53, 27–62.

Hou, Z.Q., Gao, Y.F., Meng, X.L., Qu, X.M., Huang, M., 2004. Genesis of adakitic porphyry and tectonic controls on the Gangdese Miocene porphyry copper belt in the Tibetan orogeny. Acta Geol. Sin. 20 (2), 239–248.

Hou, Z.Q., Pan, X.F., Li, Q.Y., Yang, Z.M., Song, Y.C., 2013. The giant Dexing porphyry Cu–Mo–Au deposit in east China: product of melting of juvenile lower crust in an intracontinental setting. Mineral. Deposita 48, 1019–1045.

Huang, F., He, Y.S., 2010. Partial melting of the dry mafic continental crust: implications for petrogenesis of C-type adakites. Chin. Sci. Bull. 55 (22), 2428–2439.

Irvine, T.N., Baragar, W.R.A., 1971. A guide to the chemical classification of the common volcanic rocks. Can. J. Earth Sci. 8, 523–548.

Jiang, N., Liu, Y.S., Zhou, W.G., Yang, J.H., Zhang, S.Q., 2007. Derivation of Mesozoic adakitic magmas from ancient lower crust in the North China craton. Geochim. Cosmochim. Acta 71 (10), 2591–2608.

Kay, R.W., 1978. Aleutian magnesian andesites: melts from subducted Pacific Ocean crust. Journal Volcanology and Geothermal Research 4, 117–132.

Kay, R.W., Kay, S.M., 1993. Delamination and delamination magmatism. Tectonophysics 219, 177–189.

Keith, J.D., Whitney, J.A., Hattori, K., Ballantyne, G.H., Christiansen, E.H., Barr, D.L., Cannan, T.M., Hook, C.J., 1997. The role of magmatic sulfide and mafic alkaline magmas in the Bingham and Tintic Mining Districts, Utah. J. Petrol. 38, 1679–1690.

Kelemen, P.B., 1995. Genesis of high Mg# andesites and the continental crust. Contrib. Mineral. Petrol. 120, 1–19.

Kelemen, P.B., Hart, S.R., Bernstein, S., 1998. Silica enrichment in the continental upper mantle via melt/rock reaction. Earth Planet. Sci. Lett. 164, 387–406.

Kelemen, P.B., Hanghøj, K., Greene, A.R., 2003. One view of the geochemistry of subduction-related magmatic arcs, with an emphasis on primitive andesite and lower crust. Treatise on Geochemistry 3, 593–659.

Kent, A.J.R., Darr, C., Koleszar, A.M., Salisbury, M.J., Cooper, K.M., 2010. Preferential eruption of andesitic magmas through recharge filtering. Nat. Geosci. 3 (9), 631–636.

Le Maitre, R.W., 1989. A Classification of Igneous Rocks and Glossary of Terms. Blackwell, Oxford, pp. 1–193.

Leslie, R.A., Danyushevsky, L.V., Crawford, A.J., Verbeeten, A.C., 2009. Primitive shoshonites from Fiji: geochemistry and source components. Geochem. Geophys. Geosyst. 10 (7), 1–24.

Li, Z.X., Li, X.H., 2007. Formation of the 1300-km-wide intracontinental orogen and postorogenic magmatic province in Mesozoic South China: a flat-slab subduction model. Geology 35, 179–182.

Li, X.H., McCulloch, M.T., 1996. Secular variation on the Nd isotopic composition of Neoproterozoic sediments from the southern margin of the Yangtze block: evidence for a Proterozoic continental collision in southeast China. Precambrian Res. 76, 67–76.

Li, J.W., Zhao, X.F., Zhou, M.F., Vasconcelos, P., Ma, C.Q., Deng, X.D., De Souza, Z.S., Zhao, Y.X., Wu, G., 2008. Origin of the tongshankou porphyry–skarn Cu–Mo deposit, Eastern Yangtze craton, Eastern China: geochronological, geochemical, and Sr–Nd–Hf isotopic constraints. Mineral. Deposita 43 (3), 315–336.

Li, J.W., Zhao, X.F., Zhou, M.F., Ma, C.Q., De Souza, Z.S., Vasconcelos, P., 2009. Late Mesozoic magmatism from the Daye region, eastern China: U–Pb ages, petrogenesis, and geodynamic implications. Contrib. Mineral. Petrol. 157, 383–409.

Li, X.H., Li, W.X., Wang, X.C., Li, Q.L., Liu, Y., Tang, G.Q., Gao, Y.Y., Wu, F.Y., 2010. SIMS U-Pb zircon geochronology of porphyry Cu-Au-(Mo) deposits in the Yangtze River Metallogenic Belt, eastern China: magmatic response to early Cretaceous lithospheric extension. Lithos 119, 427–438.

Li, X.H., Li, Z.X., Li, W.X., Wang, X.C., Gao, Y., 2013. Revisiting the "C-type adakites" of the Lower Yangtze River Belt, central eastern China: in-situ zircon Hf-O isotope and geochemical constraints. Chem. Geol. 345 (1), 1–15.

Liao, K.Z., Morton, D.M., Lee, C.T.A., 2013. Geochemical diagnostics of metasedimentary dark enclaves: a case study from the peninsular ranges batholith, southern California. Int. Geol. Rev. 55 (9), 1049–1072.

Ling, M.X., Wang, F.Y., Ding, X., Hu, Y.H., Zhou, J.B., Zartman, R.E., Yang, X.Y., Sun, W.D., 2009. Cretaceous ridge subduction along the Lower Yangtze River Belt, eastern China. Econ. Geol. 104, 303–321.

Liu, K., Zhang, J.J., Wilde, S.A., Zhou, J.B., Wang, M., Ge, M.H., Wang, J.M., Ling, Y.Y., 2017. Initial subduction of the Paleo-Pacific Oceanic plate in NE China: constraints from whole-rock geochemistry and zircon U-Pb and Lu-Hf isotopes of the Khanka Lake granitoids. Lithos 274, 254–270.

Ma, Q., Zheng, J.P., Xu, Y.G., Griffin, W.L., Zhang, R.S., 2015. Are continental “adakites” derived from thickened or foundered lower crust? Earth Planet. Sci. Lett. 419, 125–133.

Ma, Q., Xu, Y.G., Deng, Y.F., Zheng, J.P., Sun, M., Griffin, W.L., Xia, B., Wang, C.Y., 2019. Similar crust beneath disrupted and intact cratons: arguments against lower-crust delamination as a decratonization trigger. Tectonophysics 750, 1–8.

Maas, R., Nicholls, I.A., Legg, C., 1997. Igneous and metamorphic enclaves in the S-type Deddick granodiorite, Lachlan Fold Belt, SE Australia: petrographic, geochemical and Nd-Sr isotopic evidence for crustal melting and magma mixing. J. Petrol. 38(7), 815–841.

Mao, J.W., Xie, G.Q., Duan, C., Pirajno, F., Ishiyama, D., Chen, Y.C., 2011. A tectono- genetic model for porphyry–skarn-stratabound Cu–Au–Mo–Fe and magnetite–apatite deposits along the Middle–Lower Yangtze River Valley, Eastern China. Ore Geol. Rev. 43, 294–314.

Martin, H., Smithies, R.H., Rapp, R., Moyen, J.F., Champion, D., 2005. An overview of adakite, tonalite-trondhjemite-granodiorite (TTG), and sanukitoid: relationships and some implications for crustal evolution. Lithos 79, 1–24.

Moyen, J., 2009. High Sr/Y and La/Yb ratios: the meaning of the "adakitic signature". Lithos 112 (3–4), 556–574.

Mungall, J.E., 2002. Roasting the mantle: slab melting and the genesis of major Au and Au-rich Cu deposits. Geology 30, 915–918.

Müntener, O., Ulmer, P., 2006. Experimentally derived high-pressure cumulates from hydrous arc magmas and consequences for the seismic velocity structure of lower arc crust. Geophys. Res. Lett. 33, L21308.

Müntener, O., Kelemen, P.B., Grove, T.L., 2001. The role of H_2O during crystallization of primitive arc magmas under uppermost mantle conditions and genesis of igneous pyroxenites: an experimental study. Contrib. Mineral. Petrol. 141, 643–658.

Oyarzún, R., Márquez, A., Lillo, J., López, I., Rivera, S., 2001. Giant versus small porphyry copper deposits of cenozoic age in northern Chile: adakitic versus normal calc-alkaline magmatism. Mineral. Deposita 36, 794–798.

Pan, Y.M., Dong, P., 1999. The lower Yangtze (Yangtze/Changjiang) metallogenic belt, east central China: intrusion- and wall rock-hosted Cu-Fe-Au, Mo, Zn, Pb, Ag deposits. Ore Geol. Rev. 15, 177–242.

Patriat, M., Falloon, T.J., Danyushevsky, L.V., Collot, J., Jean, M.M., Hoernle, K., Hauff, F., Maas, R., Woodhead, J.D., Feig, S.T., 2019. Subduction initiation terranes exposed at the front of a 2 Ma volcanically-active subduction zone. Earth Planet. Sci. Lett. 508, 30–40.

Peccerillo, A., Taylor, S.R., 1976. Geochemistry of Eocene calkalkaline volcanic rocks fromthe Kastamonu area, northern Turkey. Contrib. Mineral. Petrol. 58, 61–83.

Plank, T., 2005. Constraints from thorium/lanthanum on sediment recycling at subduction zones and the evolution of the continents. J. Petrol. 46 (5), 921–944.

Plank, T., Langmuir, C.H., 1998. The chemical composition of subducting sediment and its consequences for the crust and mantle. Chem. Geol. 145, 325–394.

Qian, Q., Hermann, J., 2013. Partial melting of lower crust at 10–15 kbar: constraints on adakite and TTG formation. Contrib. Mineral. Petrol. 165 (6), 1195–1224.

Qiu, Y.M., Gao, S., McNauthton, N.J., Groves, D.I., Ling, W.L., 2000. First evidence of >3.2 Ga continental crust in the Yangtze craton of South China and its implications for Archean crustal evolution and Phanerozoic tectonics. Geology 28, 11–14.

Rapp, R.P., Watson, E.B., 1995. Dehydration melting of metabasalt at 8–32 kbar: implications for continental growth and crust-mantle recycling. J. Petrol. 36, 891–931.

Rapp, R.P., Shimizu, N., Norman, M.D., 2003. Growth of early continental crust by partial melting of eclogite. Nature 425, 605–609.

Richards, J.R., Kerrich, R., 2007. Special paper: adakite-like rocks: their diverse origins and questionable role in metallogenesis. Econ. Geol. 102, 537–576.

Schiano, P., Monzier, M., Eissen, J.P., Martin, H., Koga, K.T., 2010. Simple mixing as the major control of the evolution of volcanic suites in the Ecuadorian Andes. Contrib. Mineral. Petrol. 160, 297–312.

Schmidt, M.W., Dardon, A., Chazot, G., Vannucci, R., 2004. The dependence of Nb and Ta rutile-melt partitioning on melt composition and Nb/Ta fractionation during subduction processes. Earth Planet. Sci. Lett. 226, 415–432.

Shu, Q.A., Chen, P.R., Chen, J.R., 1992. Geology of Fe–Cu ore deposits in Eastern Hubei Province. Press of Metallurgical Industry, Beijing 532.

Snyder, D., Tait, S., 1998. The imprint of basalt on the geochemistry of silicic magmas. Earth Planet. Sci. Lett. 160, 433–445.

Sun, S.S., McDonough, W.F., 1989. Chemical and isotopic systematics of oceanic basalts: implications for mantle composition and processes. In: Saunders, A.D., Norry, M.J. (Eds.), Implications for Mantle Composition and Processes, Magmatism in the Ocean Basins. Geological Society, London, Special Publication 42, pp. 313–345.

Sun, J.F., Yang, J.H., Wu, F.Y., Li, X.H., Yang, Y.H., Xie, L.W., Wilde, S.A., 2010. Magma mixing controlling the origin of the Early Cretaceous Fangshan granitic pluton, North China Craton: in situ U–Pb age and Sr-, Nd-, Hf- and O-isotope evidence. Lithos 120 (3–4), 421–438.

Takahashi, Y., Kagashima, S.I., Mikoshiba, M.U., 2005. Geochemistry of adakitic quartz diorite in the Yamizo Mountains, central Japan: implications for Early Cretaceous adakitic magmatism in the inner zone of southwest Japan. Island Arc 14, 150–164.

Tasumi, Y., Hamilton, D.L., Nesbitt, R.W., 1986. Chemical characteristics of fluid phase released from a subducted lithosphere and the origin of arc magmas: evidence from high pressure experiments and natural rocks. Journal Volcanology and Geothermal Research 29, 293–309.

Tindle, A.G., Pearce, J.A., 1983. Assimilation and partial melting of continental crust: evidence from the mineralogy and geochemistry of autoliths and xenoliths. Lithos 16, 185–202.

Treuil, M., Joron, J.M., 1975. Vtilisation des element hydromagmatophiles pour la simplification de la modelisation quantitative des proccessus magmatiques, Examples de'l afar et de la dorsade medioatlatipue. Soc. It. Mine. Petrol. 31, 125.

Tulloch, A.J., Kimbrough, D.L., 2003. Paired plutonic belts in convergent margins and the development of high Sr/Y magmatism: peninsular ranges batholith of Baja-California and Median batholith of New Zealand. Geol. Soc. Am. Spec. Pap. 374, 1–21.

Turner, S., Arnaud, N., Liu, J., Rogers, N., Hawkesworth, C., Harris, N., Kelley, S., Van Calsteren, P., Deng, W., 1996. Post-collision, shoshonitic volcanism on the Tibetan Plateau: implications for convective thinning of the lithosphere and the source of ocean island basalts. J. Petrol. 37 (1), 45–71.

Vernon, R.H., 1983. Restite, xenoliths and microgranitoid enclaves in granites. J. Proc. R. Soc. NSW 116, 77–103.

Vernon, R.H., 1984. Microgranitoid enclaves in granites; globules of hybrid magma quenched in a plutonic environment. Nature 309, 438–439.

Wang, J.L., He, B., 2016. LA-ICP-MS U-Pb Dating of Detrital Zircons from Dongling Group in Hongzhen Area and its Geological Implications. Geotecton. Metallog. 40 (6), 1239–1246.

Wang, Q., Zhao, Z.H., Xu, J.F., Li, X.H., Bao, Z.W., Xiong, X.L., Liu, Y.M., 2003. Petrogenesis and metallogenesis of the Yanshanian adakite-like rocks in the Eastern Yangtze Block. Sci. China Ser. D Earth Sci. 46 (1), 164–176.

Wang, Q., Zhao, Z.H., Bao, Z.W., Xu, J.F., Liu, W., Li, C.F., Bai, Z.H., Xiong, X.L., 2004. Geochemistry and petrogenesis of the Tongshankou and Yinzu adakitic intrusive rocks and the associated porphyry copper–molybdenum mineralization in southeast Hubei, east China. Resour. Geol. 54, 137–152.

Wang, Q., Wyman, D.A., Xu, J.F., Zhao, Z.H., Jian, P., Xiong, X.L., Bao, Z.W., Li, C.F., Bai, Z.H., 2006. Petrogenesis of Cretaceous adakitic and shoshonitic igneous rocks in the Luzong area, Anhui Province (eastern China): implications for geodynamics and Cu–Au mineralization. Lithos 89, 424–446.

Wang, Q., Wyman, D.A., Xu, J.F., Jian, P., Zhao, Z.H., Li, C.F., Xu, W., Ma, J.L., He, B., 2007. Early Cretaceous adakitic granites in the Northern Dabie Complex, central China: implications for partial melting and delamination of thickened lower crust. Geochim. Cosmochim. Acta 71 (10), 2609–2636.

Wang, S.W., Zhou, T.F., Yuan, F., Fan, Y., Cooke, D.R., Zhang, L.J., Fu, B., White, N.C., 2016. Geochemical characteristics of the Shujiadian Cu deposit related intrusion in Tongling: Petrogenesis and implications for the formation of porphyry Cu systems in the Middle–Lower Yangtze River Valley metallogenic belt, eastern China. Lithos 252, 185–199.

Wyllie, P.L., Cox, K.G., Biggar, G.M., 1962. The habit of apatite in synthetic systems and igneous rocks. Petrology 3 (2), 238–243.

Xia, J.L., Huang, G.C., Ding, L.X., Cheng, S.B., 2015. In situ analyses of trace elements, U–Pb and Lu–Hf isotopes in zircons from the Tongshankou granodiorite porphyry in southeast Hubei province, middle-lower Yangtze River metallogenic belt, China. Acta Geol. Sin. 89 (5), 1588–1600.

Xie, G.Q., Mao, J.W., Li, R.L., Zhou, S.D., Ye, H.S., Yan, Q.R., Zhang, Z.S., 2006. SHRIMP zircon U-Pb dating for volcanic rocks of the Dasi Formation in southeast Hubei Province, middle-lower reaches of the Yangtze River and its implications. Chin. Sci. Bull. 51 (24), 3000–3009.

Xie, G.Q., Mao, J.W., Li, R.L., Beirlein, F.P., 2008. Geochemistry and Nd–Sr isotopic studies of Late Mesozoic granitoids in the southeastern Hubei province, Middle–Lower Yangtze River belt, Eastern China: petrogenesis and tectonic setting. Lithos 104, 216–230.

Xie, G.Q., Mao, J.W., Li, X.W., Duan, C., Yao, L., 2011a. Late Mesozoic bimodal volcanic rocks in the Jinniu basin, Middle–Lower Yangtze River Belt (YRB), East China, Age, petrogenesis and tectonic implications. Lithos 127, 144–164.

Xie, G.Q., Mao, J.W., Zhao, H.J., 2011b. Zircon U-Pb geochronological and Hf isotopic constraints on petrogenesis of late Mesozoic intrusions in the Southeast Hubei Province, Middle-Lower Yangtze River belt (MLYRB), East China. Lithos 125, 693–710.

Xie, G.Q., Mao, J.W., Zhao, H.J., Wei, K.T., Jin, S.G., Pan, H.J., Ke, Y.F., 2011c. Timing of skarn deposit formation of the Tonglushan ore district, southeastern Hubei Province, Middle-Lower Yangtze River Valley metallogenic belt and its implications. Ore Geol. Rev. 43, 62–77.

Xu, Y.G., 2001. Thermo-tectonic destruction of the Archaean lithospheric keel beneath the Sino-Korean Craton in China: evidence, timing and mechanism. Phys. Chem. Earth Solid Earth Geod. 26, 747–757.

Xu, X., Xing, F.M., 1994. Whole rocks and Mineral. Rb–Sr isochron ages of the three gabbros in Nanjing-Wuhu area, China. Sci. Geol. Sin. 29, 309–312 (in Chinese with English abstract).

Xu, J.F., Shinjo, R., Defant, M.J., Wang, Q.A., Rapp, R.P., 2002. Origin of Mesozoic adakitic intrusive rocks in the Ningzhen area of East China: partial melting of delaminated lower continental crust? Geology 30, 1111–1114.

Yan, J., Chen, J.F., Xu, X.S., 2008. Geochemistry of Cretaceous mafic rocks from the Lower Yangtze region, eastern China: Characteristics and evolution of the lithospheric mantle. J. Asian Earth Sci. 33, 177–193.

Yan, D.R., Deng, X.D., Hu, H., Li, J.W., 2012. U-Pb age and petrogenesis of the Ruanjiawan granodiorite pluton and Xiniushan granodiorite porphyry, Southeast Hubei Province: implications for Cu-Mo mineralization. Acta Geol. Sin. 28 (10), 3373–3388.

Yogodzinski, G.M., Volynets, O.N., Koloskov, A.V., Seliverstov, N.I., Matvenkov, V.V., 1994. Magnesian andesites and the subduction component in a strongly calc-alkaline series at Piip Volcano, Far Western Aleutians. J. Petrol. 35, 163–204.

Yogodzinski, G.M., Kay, R.W., Volynets, O.N., Koloskov, A.V., Kay, S.M., 1995. Magnesian andesite in the western Aleutian Komandorsky region: Implications for slab melting and processes in the mantle wedge. Geol. Soc. Am. Bull. 107, 505–519.

Yuan, F., Zhou, T.F., Fan, Y., Lu, S.M., Qian, C.C., Zhang, L.J., Duan, C., Tang, M.H., 2008. Source, evolution and tectonic setting of Mesozoic volcanic rocks in Luzong basin, Anhui Province. Acta Geol. Sin. 24, 1691–1702.

Zhai, Y.S., Yao, S.Z., Lin, X.D., Zhou, X.R., 1992. Metallogeny of Fe–Cu–(Au) Ore deposits in mid-lower Changjiang. *Geological Publishing House, Beijing*, p 198(in Chinese with English Abstract).

Zhai, Y.S., Xiong, Y.L., Yao, S.Z., Lin, X.D., 1996. Metallogeny of copper and iron deposits in the Eastern Yangtse Craton, east-central China. Ore Geol. Rev. 11, 229–248.

Zhang, S.T., Chen, H.Y., Han, J.S., Zhang, Y., Chu, G.B., Wei, K.T., Zhao, Y.J., Cheng, J.M., Tian, J., 2018. Geochronology, geochemistry and mineralization of the quartz monzodiorite and quartz monzodiorite porphyry in the Tonglvshan Cu-Fe-Au deposit, Edongnan ore district, China. Geochimica 47 (03), 240–256.

Zhao, H.J., Mao, J.W., Xiang, J.F., Zhou, Z.H., Wei, K.T., Ke, Y.F., 2010. Mineralogy and Sr–Nd–Pb isotopic compositions of quartz diorite in Tonglushan deposit, Hubei Province. Acta Geol. Sin. 26, 768–784.

Zhao, K.D., Jiang, S.Y., Yang, S.Y., Dai, B.Z., Lu, J.J., 2012. Mineral chemistry, trace elements and Sr–Nd–Hf isotope geochemistry and petrogenesis of Cailing and Furong granites and mafic enclaves from the Qitianling batholith in the Shi-Hang zone, South China. Gondwana Res. 22 (1), 310–324.

Zheng, J.P., Lee, C.T.A., Lu, J.G., Zhao, J.H., Wu, Y.B., Xia, B., Li, X.Y., Zhang, J.F., Liu, Y.S., 2015. Refertilization-driven destabilization of subcontinental mantle and the importance of initial lithospheric thickness for the fate of continents. Earth Planet. Sci. Lett. 409, 225–231.

Zhou, X.M., Li, W.X., 2000. Origin of Late Mesozoic igneous rocks in southeast China: implications for lithosphere subduction and underplating of mafic magmas. Tectonophysics 326 (3–4), 269–287.

Zhou, T.F., Fan, Y., Yuan, F., Lu, S.M., Shang, S.G., Cooke, D., Meffre, S., Zhao, G.C., 2008. Geochronology of the volcanic rocks in the Lu-Zong basin and its significance. Sci. China Ser. D Earth Sci. 51 (10), 1470–1482.

Zhou, T.F., Wang, S.W., Fan, Y., Yuan, F., Zhang, D.Y., White, N.C., 2015. A review of the intracontinental porphyry deposits in the Middle-Lower Yangtze River Valley metallogenic belt, Eastern China. Ore Geol. Rev. 65, 433–456.

Zindler, A., Hart, S.R., 1986. Chemical geodynamics. Annu. *Rev. Earth Planet. Sci.* 14 (1), 493–571.